中 國 醫 藥 大 學
生物科技系碩士班
碩士學位論文

由 NCI 資料庫虛擬篩選 H1N1, H1N2 與 H1N7 之多靶點藥物

Multiple-target drug design for H1N1, H1N2, and H1N7 by virtual screening the NCI database

指 導 教 授 ：陳語謙　教　授

研 究 生：陳建宇

中 華 民 國 九 十 八 年 七 月

中文摘要

在 2009 年初，H1N1 流感疫情自墨西哥爆發並擴至全世界，因此開發新型抑制劑來對抗此波疫情已是燃眉之急。在本研究中，我們使用目前最新的 H1N1 序列以同源模擬法模擬出目前為止最新的 H1 與 N1 的蛋白質結構。由 Ramachandran 圖可知，在 H1 結構上僅有 1.28% 落於非合理角度構型的區域上；在 N1 結構上也僅有 3.4%。加上 Verify Score plot 判讀得知，H1 與 N1 的模擬結構有相當高的可信度。NCI 資料庫包含有 365,602 個已知結構的藥用化合物，在本研究中以虛擬篩選的方式由其中選出具有潛力的化合物：NCI0624650, NCI0607158, NCI0605741, PROTOVERINE, NCI0605737 KANAMYCIN-C, NCI0608643, NCI0606258, and NCI0608650 等九種。除此之外，新的 N1 結構在此虛擬平台上被發現對於 oseltamivir 具有抗藥性。另一方面我們也以 N2 與 N7 的蛋白質結構個別生成了藥效基團的交互作用圖，並與 N1 的藥效基團假設做比對，在此研究中探討了三者的差異，完成了混合型藥效基團模型。最後以此混合型藥效基團模型用以篩選 NCI 資料庫，找出了六個可能成為廣效性 NA 抑制劑的候選化合物。我們的研究對於 H1N1 當前之疫情控制及未來之疫情預防，都有指標性的貢獻。

關鍵字： H1N1，虛擬篩選，建構藥效基團假設，廣效性抑制劑

Abstract

An outbreak of H1N1 influenza in Mexico was occurred in 2009. To find out drugs for treating this epidemic is emergency. In this study, we have built the latest N1 and H1 structure model by homology modeling, which has high reliability by Verify Score plot. In Ramachandran plot, it shows only 1.28% and 3.4% out of the region of possible angle formations in N1 and H1 models, respectively. 365,602 compounds from NCI database have been screened by docking study of H1 and N1, respectively. And then, NCI0624650, NCI0607158, NCI0605741, PROTOVERINE, NCI0605737 KANAMYCIN-C, NCI0608643, NCI0606258, and NCI0608650 were suggested as potent dual target candidates from the docking studies. Moreover, the latest N1 structure was found that have drug resistance to oseltamivir. Additionally, we have also created the interaction maps in the active sites on the neuraminidase type2, and type7 (N2 and N7) protein structures, aiming at creating the combined map for N1, N2, and N7 to resolve the difference in the three NA types. The combined map was employed to NCI database screening, and 6 candidates were found to be useful potent versatile inhibitors for N1, N2 and N7.

Key words： neuraminidase, virtual screening, pharmacophore hypothesis generation (HyPoGen), versatile inhibitor

致謝

在碩士兩年的學習過程，隨著論文的付梓，即將劃上句點。本論文能順利完成，幸蒙指導教授-陳語謙老師的指導與教誨，對於研究的方向、觀念的啟迪、架構的匡正、資料的提供與求學的態度逐一斧正與細細關懷，於此獻上最深的敬意與謝意。論文口試期間，承蒙口試委員包大牖老師與吳正男老師的鼓勵與疏漏處之指正，使得本論文更臻完備，在此謹深致謝忱。在研究所修業期間，感謝鍾景光主任在行政事務的協助。感謝蔡輔仁院長與蔡長海董事在實驗上的支援。感謝侯庭鏞老師在中草藥研究上的啟發、感謝簡惠玲老師指導論文的寫作以及徐媛曼老師在課業上的解惑，獲益良多。紹貴學長在學業與實驗上的指導與泓縉學弟在實驗繁忙時的幫忙協助，永難忘懷。感謝國家高速網路計算中心提供高速計算的環境，使本研究計算的資料庫篩選能夠順利完成。對於所有幫助過我、關懷過我的人，致上由衷感謝。最後，特將本文獻給我最敬愛的父母，感謝您無怨無悔的養育與無時無刻的關懷照顧，以及在經濟上與精神上的支持，讓我能專注於課業研究中，願以此與家人共享。

總目錄

表目錄

圖目錄

1. 簡介(Introduction)

The membranes of influenza virus contain haemagglutinin (HA) and neuraminidase (NA), they both are glycoproteins. Haemagglutinin has 16 subtypes (H1, H2, H3,…H16) and neuraminidase has 9 subtypes (N1, N2, N3,…N9). They assort the type of influenza A viruses (Mukhtar *et al*., 2007; Shirvan *et al*., 2007). Binding of cell-surface sialic acid receptor to initiate virus was mediates by HA, and sialic acid was removed from virus by NA. By the two steps, cellular glycoproteins improve virus releasing and the spread of infection to new cells, respectively (Raymond and Leach, 2007; Takabatake *et al*., 2007). To block haemagglutinin or neuraminidase also could prevent virus from invading into host cells (Russell *et al*., 2006; Shimbo *et al*., 2007). Zanamivir (Relenza) and oseltamivir (Tamiflu) both are neuraminidase inhibitors (Ho *et al*., 2007; Collins *et al*., 2008). Influenza A virus subtype H1N1 is the most common cause of influenza in human (Palese, 2004). Some strains of H1N1 are human endemic; such as the pandemic flu in 1918, 50-100 million people were killed worldwide (Kash *et al*., 2006; Kobasa *et al*., 2007). Less virulent H1N1 strains which roughly caused half of flu

infections in 2006 has still existed (Cheung *et al*., 2002; Palese, 2004; Kash *et al*., 2006; Kobasa *et al*., 2007); other strains of H1N1 in swine and fowls are endemic. Since March 2009, an outbreak of H1N1 influenza in Mexico has led to hundreds of confirmed cases and a number of deaths. On April 28, the new strain was suspected the infection more than 2,500 individuals worldwide and 152 attributed deaths. The U.S. Centers for Disease Control and Prevention warned that the outbreak could be pandemic. On April 27, 2009, the World Health Organization raised their alertness level from 3 to 4 worldwide in response to sustain human-to-human transfer of the virus, and the situation was raised to level 5 on April 29. There is an urgent need to find the resolution for this international problem. Unfortunately, H1N1 virus was reported that has gained drug resistant for oseltamivir (Collins *et al*., 2008; Hauge *et al*., 2009; Moscona, 2009). Hence, a new emergent drug is needed to against this epidemic. In the past few years, many reports indicated that virtual screening techniques were feasible (Chen, 2008a,b,c,d; Chen, 2009a,b,c). In this study, we have built the H1 and N1 structure model by homology modeling. Homology modeling, hypothesis generation, and docking analysis were employed in our experiment for this research. A dual target

research was carried out by the protocols for H1 and N1. 365,602 compounds from NCI database have been screened by docking study of H1 and N1, respectively. Additionally, we created the interaction maps in the active sites on the neuraminidase type2, and type7 (N2 and N7) protein structures. The structure-based pharmacophore map showed the features on every amino acid in the active site on the protein structure. By pharmacophore comparison, root-mean-squared error (RMSE) was reported for the matching pharmacophore features. We aimed at figuring out potent candidates for N1 and H1 for the 2009 outbreak of influenza A H1N1.

2. 方法與材料(Material and methods)

2-1 資料設定(Data set)

All programs in this study were performed by Discovery Studio 2.0 (Accelrys, San Diego, CA, USA). The latest sequences of H1 and N1 were downloaded from NCBI influenza virus sequence database. The templates of H1 and N1 were downloaded from protein data bank (PDB). Their structures had been released in 2004 and 2006, respectively. (PDB ID: 1RD8 and 2HU0) (Stevens *et al*., 2004; Russell *et al*., 2006) The multiple sequence alignment method was based on the CLUSTAL W program and progressive pairwise alignment algorithm (Thompson *et al*., 1994). The alignment scoring matrix was set in BLOSM via default. We applied 1RD8 and 2HU0 to build the latest structure of the H1 and N1 sequence, respectively. The structures of 18 nureaminidase inhibitors were obtained from Lu's study (Table 1) (Lu *et al*., 2008). The concentration of inhibitor that produces 50% inhibition of nureaminidase (IC50) was used in pharmacophore hypotheses and structure-activity relationship (SAR) study.

2-2 建構藥效基團假設(Pharmacophore hypotheses generation,

HyPoGen)

HyPoGen constructs pharmacophore hypotheses by using an informative training set that includes over 16 molecules with bioactivities. Accordingly, 18 compounds (Lu *et al*., 2008) were selected in training set for generating 10 pharmacophore hypotheses (Table 1 and 2). The hypotheses were accepted by those conditions: the null cost subtracted total cost was over 60, the configure value should be less than 17, and a high correlation between actual active values and fit values (Kurogi and Guner, 2001; Bersuker *et al*., 2000).

HyPoGen was built by three steps: Constructive phase, Subtractive phase, and Optimization phase (Kurogi *et al*., 2001; Bersuker *et al*., 2000). In constructuive phase, the fixed hypothesis was built by the features of the most active compound. The maximum number of features were limited as 5. Other active compounds (principal = 2, Tabel 2.) were requested to satisfy following equation:

$$(\mathrm{MAct} \times \mathrm{UncMAct}) - (\mathrm{Act} / \mathrm{UncAct}) > 0.0 \quad \text{...(1)}$$

MAct was the highest activ value in the data set. Unc was the uncert value. Act was the activ value in the data set (Table 2.). The features of compounds, which satisfied Eq. 1, were employed to develop pharmacophore hypotheses. In subtractive phase, the most inactive

compound was used to form a pharmacophore hypothesis. Other inactive compounds (principal = 0, Table 2.) were requested to satisfy following equation:

$$\log(\text{Act}) - \log(\text{MAct}) > 3.5 \quad \text{.....(2)}$$

The features of compounds, which satisfied Eq. 2, were employed to construct the null hypothesis. Those features were considered as factors decreasing activities of compounds and eliminated from pharmacophore hypothese. In optimization phase, HypoGen applies small perturbation to the pharmacophores created in constructive and subtractive phases in an attempt to improve the score. The steps includes selecting a new pharmacophore from the list of possibilities, rotating a vectored feature, translating a randomly selected feature in the pharmacophore, adding a new features, and removing a feature. For a particular hypothesis, the activities of compounds are estimated through the equation as following (Kurogi and Guner, 2001; Bersuker *et al*., 2000):

$$\log(\text{Estimated activity}) = I + \text{Fit} \quad \text{.....(3)}$$

Where *I* is the intercept of the regression line, which is generated by plotting. The log of the biological activities of the data set molecules against the Fit values of them. The Fit values are estimated through the

equation as following (Kurogi and Guner, 2001; Bersuker *et al*., 2000):

$$\text{Fit} = \sum \text{mapped hypothesis features} \times W\left[1 - \sum (\text{disp}/\text{tol})^2\right] \quad \text{.....(4)}$$

Where $\sum$ mapped hypothesis features is the successfully superimposed pharmacophore feature number, W is the weight of the corresponding hypothesis feature spheres, disp is the distance between the feature centroid and the center of the corresponding superimposed chemical moiety of the fitted molecule, tol is the radius of the pharmacophore feature sphere (tolerance, 1.6 Å by default). The confidence level of 95% was generated from 19 random spreadsheets by Cat-Scramble program in each modeling run (Kurogi *et al*., 2001).

2-3 NCI 資料庫之篩選(NCI database screening)

NCI database was provided by National Center for High-performance Computing. The database included 365,602 compounds. We employed the first pharmacophore hypothesis to map and aligned the compounds from NCI database by the Catalyst compare/fit algorithm. The log of the biological activities of the data set molecules was against the Fit values. The Fit values are estimated by Eq. 4. Tolerance was set 1.6 Å by default.

2-4 分子對接分析(Molecular docking study)

All of the compounds were built and energy minimized under MM2 force field by ChemOffice 2005. The LigandFit program performed the docking simulation at the binding site by Discovery Studio 2.0. During the docking procedure, ligands were flexible whereas the receptor was fixed. The ligand flexibility was carried out by In-Situ Ligand Minimization based on CHARMm force field. Docking score (D.S.) was employed to score the docking results. Candidate ligand poses are evaluated and prioritized according to the DockScore function. There are three types of DockScore. One is based on a forcefield approximation, another on the Piecewise Linear Potential function (PLP), and Potential of Mean Force (PMF).

DockScore(forcefield) = - (ligand/receptor interaction energy + ligand internal energy)……...(5)

As shown in Eq. 5, there are two energy terms in the forcefield version of DockScore, internal energy of the ligand and the interaction energy of the ligand with the receptor. The interaction energy is taken as the sum of the van der Waals energy and electrostatic energy. The computation of the interaction energy can be quite time consuming. To reduce the time needed for this calculation, a grid-based estimation of the

ligand/receptor interaction energy is employed.

Piecewise Linear Potential is a fast, simple, docking function that has been shown to correlate well with protein-ligand binding affinities. PLP scores are measured in arbitrary units, with negative PLP scores reported in order to make them suitable for subsequent use in consensus score calculations.

DockScore(PLP) = - (PLPpotential)……...……(6)

Higher PLP scores indicate stronger receptor-ligand binding (larger pK_i values). Two versions of the PLP function are available: PLP1 (Gehlhaar *et al.*, 1995) and PLP2 (Gehlhaar *et al.*, 1999). In the PLP1 function, each non-hydrogen ligand or non-hydrogen receptor atom is assigned a PLP atom type. Hydrogens are excluded from consideration. There are four PLP atom types:

1. Hydrogen bond (H-bond) donor only.
2. H-bond acceptor only.
3. Both H-bond donor and acceptor.

Non-pola There are two types of pairwise interactions in PLP1 as shown in Table 3, namely H-bond and steric. The two interactions are described by the same functional form, but with different parameters

(Figure 1 and Table 4). The PLP1 score is the sum of the function values of all pairwise interactions in a receptor-ligand complex.

In the PLP2 function, PLP atom typing remains the same as in PLP1. In addition, an atomic radius is assigned to each atom except for hydrogen. There are three different radii:

1. Small: a value of 1.4 for F and metal ions (including Zn, Mn, Mg, and Fe).
2. Medium: a value of 1.8 for C, O, and N.
3. Large: a value of 2.2 for S, P, Cl, and Br.

There are three types of pairwise interactions in PLP2 as shown in Table 5, namely H-bond, dispersion, and repulsion. There are two types of functional forms. The H-bond and dispersion interactions have the same functional form, but different parameters (Figure 2 and Table 6). A scaling factor is used for H-bond and repulsion terms based on the angle formed by the corresponding receptor-ligand atoms. The PLP2 score is the sum of the function values of all pairwise interactions in a receptor-ligand complex.

The PMF scoring functions were developed based on statistical analysis of the 3D structures of protein-ligand complexes. They were

found to correlate well with protein-ligand binding free energies while being fast and simple to calculate. The scores are calculated by summing pairwise interaction terms over all interatomic pairs of the receptor-ligand complex (Muegge and Martin, 1999). The PMF scores are reported in arbitrary units with the sign reversed to allow for subsequent use in consensus score calculations. A higher score indicates a stronger receptor-ligand binding affinity. Otherwise, the Consensus Score (CS) protocol calculates the consensus scores of a series of docked ligands for which other scores have been previously computed. For each selected scoring function, the ligands are listed by score in descending order. The consensus scores for each molecule were employed to be a view for ranking compounds (Teramoto and Fukunishi, 2008).

2-5 藥效基團交互作用關係之生成與比對(Interaction generation and pharmacophore comparison)

The protocol enumerates pharmacophore features from a protein active site. It uses the de novo design method Ludi to create an interaction map in a protein active site. The information from the map is then converted to pharmacophore features (acceptors, donors, and

hydrophobes). The density of lipophilic sites and density of polar sites were set 25 by default. The two pharmacophores are aligned by comparison analysis. The analysis uses the Catalyst Compare/fit algorithm to map and align two pharmacophores. Root-mean-squared error (RMSE) is reported for the matching pharmacophore features.

3. 結果與討論(Results and discussion)

3-1 同源模擬之結果(The results of homology modeling)

The result of alignment was reported in Figure 3 and 4. The sequence identity is 70.8% and similarity is 78.9% in H1. On the other hand, the sequence identity and similarity of N1 sequences were 91.4% and 95.6%, respectively. Accordingly, the alignment result was employed to build homology model. The reliable result of building homology model was performed by verified score and Ramachandran plot. (Figures 5-8) The results of verified score showed that few amino acid had low score (< 0) in H1 and N1 models (Figures 5 and 6). Because the amino acids didn't locate at binding site, we thought that it could not affect the study. The Ramachandran Plot indicated low energy conformations for φ (phi) and ψ (psi), and the conventional terms represented the torsion angles on

either side of alpha carbon in peptides. This plot was used to verify the predicted torsion angles in proteins. The result of Ramachandran plot showed only 1.28% error in H1 homology modeling and 3.4% in N1 homology modeling (Figures 7 and 8).

3-2 藥效基團假設生成之結果(The results of pharmacophore hypotheses generation)

The results showed that the configuration cost value less than 17 was 11.375, and the correlation was over 0.8, which indicated the reliability of hypotheses (Table 7). The correlation of the hypothesis 2 consisted with the hypothesis 1; accordingly, the pharmacohore map of the hypothesis 1 was elevated in next calculation. Generally, the error cost 40~60 meant that the confidence level was between 75~90%. In this investigation, the confidence level was 95% to accept the hypotheses. Otherwise, the actual activity of the first hypothesis had the highest correlation (0.88) among the 10 hypotheses, which suggested the first hypothesis reflect the actual activity by structure-activity relationship (SAR). The first hypothesis showed high correlation in Figure 9. Fit values could be predicted log active values by the linear correlation (Figure 9). R value about 0.88 was calculated via R^2 = 0.7879 (Figure 9c). The first hypothesis was

constructed by two hydrogen bond acceptor features: one hydrogen bond donor feature, and one positive ionizable feature (Figure 10). The first hypothesis was consisted with the idea of designing NA inhibitor for improvement drugs activity in Shie's study (Shie *et al*., 2008). Accordingly, the first hypothesis was employed to NCI database screening. The results were showed in Table 8 and Table 9.

3-3 分子對接分析之結果(The results of docking study)

The compounds of NCI database were docked into H1 and N1 structures, respectively. The docking results of the fifty compounds with H1 were showed in Table 10. NCI0353858 had highest docking score, even higher than zanamivir and oseltamivir. In fact, zanamivir and oseltamivir were designed as inhibitors for NA. Although the results showed that zanamivir had some affinity for H1, there were many compounds more suitable than zanamivir, like NCI0353858, DESTOMYCIN-A, and NCI0607158.

In Table 11, zanamivir had 78.41 in docking score. That means zanamivir still had high activity for latest N1 in 2009. However, oseltamivir had 44.91 in docking score. In our previous study,

oseltamivir had 53.3 in docking score for N1 in 2004. The latest N1 might have drug resistance to oseltamivir, and lower the docking score of oseltamivir, outstandingly. The results were consisted with many other reports (Collins *et al*., 2008; Hauge *et al*., 2009; Moscona, 2009). PROTOVERINE and NCI0607158 had higher docking score than zanamivir in Table 11. According above, NCI0607158 was suggested as potent dual target compound. There top 9 dual-target inhibitor candidates were selected form docking results by scoring functions: NCI0624650, NCI0607158, NCI0605741, PROTOVERINE, NCI0605737 KANAMYCIN-C, NCI0608643, NCI0606258, and NCI0608650 (Figure 11). NCI0607158 was not only with docking score higher than zanamivir, but also with higher consensus score, too. We suggested that NCI0607158 might have high activity for in vitro study. The docking poses in H1 and N1 of 9 candidates were shown in Figure 12, respectively. In H1, the residuals of the binding site were like fingers to clutch the ligands by hydrogen bonds. The half-opened access shape of H1 binding site increased the difficulty for forming the ligand-pretein complex. The Table 10 showed that NCI0353858 had the highest docking score. The scores of Potential of mean force (PMF) of

NCI0605737 and NCI0608647 were higher than 70 but the dock scores were less than 50 (Table 10). PMF was computed by summing pairwise interaction terms over all interatomic pairs of the receptor-ligand complex. According to PMF scores and docking scores, NCI0353858 was suggested as a potent inhibitor. In Figure 13, hydrogen bond acceptor features were located on ASN26, GLU38, and ASN59 (Figure 13a); besides, the hydrogen bond donor features were located on SER56, GLU38, and ASP58 (Figure 13a). The hydrophobic features didn't centralize at the center of the binding site. NCI0353858 was formed with the 4 hydrogen bonds on LYS26, GLU38, ASP58, and ASN59 (Figure 13b). The results suggested that NCI0353858 should be a candidate for designing of H1 inhibitor. The first pharmacophore hypothesis developed by N1 was applied as criteria to screen NCI database. The 49 compounds were selected from the 365602 compounds by this protocol. In docking analysis, NCI0353858 which produced 4 hydrogen bonds in the ligand-protein complex was pointed out (Figure 13a and 13b). The structure of NCI0353858 was considered a lead compound for de novo drug design (Figure 13c).

Considering to increasing the binding affinity for N1, the PLP

score might play an important role in this study. PLP scores showed a trend with docking scores (Table 11). In our study, the major reason for decreasing binding affinity of oseltamivir in N1 that had low PLP score in the latest N1 structure. For improving binding affinity, extent the side chain for increasing positive charge may have effect. PROTOVERINE and NCI0607158 both had longer length than other 7 candidates (Figure 11).

3-4 N1, N2 與 N7 藥效基團比較分析之結果(Results of N1, N2, and N7 pharmacophore comparison analysis)

In this result, the binding site of N2 and N7 both showed hydrophobic core (Figure 14a and 14b). However, the hydrophobic region in the binding site of N7 was deeper than in the binding site of N2. It was suggested that drug selectivity between N2 and N7 might be created by extent C-C bonds for moving the hydrophobic group on drugs into binding site in N7 structure. The yellow circles in Figure 2b labeled the major differences between N2 and N7 interaction maps. The mount of HBA features in N7 was more than that in N2 clearly. Over addition of HBA feature on NA inhibitors may cause the activity reducing in N7. The root-mean-squared error displacement (RMSD) was reported for the

matching pharmacophore features. The total RMSD of N1-N2 comparison analysis was 0.365, and the total RMSD of N1-N7 comparison analysis was 0.451. The major error occurred at the HBA features in the tow comparison results (Table 12). This difference was thought as the different amino acids on N1, N2, and N7 structures. We suggested that distances error between maps might cause different drug activities in N1, N2, and N7. This information was though to associate with drug resistance of influenza. Additionally, the compounds from NCI database were calculated of their fit values by pharmacopore mapping to the combining map and their average docking scores by docked into the three kinds of NA. The result was shown in Table 13. It was clearly observed that the top 6 potent compounds were shown in the binding site and fitted with the combined map (Figure 15). The structures of the top 6 potent compounds were shown in Figure 16.

4. 結論(Conclusion)

In this study, we have built the latest H1 and N1 structure model by homology modeling, which has high reliability by Verify Score plot and Ramachandran plot. 365,602 compounds from NCI database have been

screened by docking study of H1 and N1, respectively. After the overall procedures presented in Fig. 1, NCI0624650, NCI0607158, NCI0605741, PROTOVERINE, NCI0605737 KANAMYCIN-C, NCI0608643, NCI0606258, and NCI0608650 (Figure 11) were suggested potent dual target candidates. Moreover, the latest N1 structure might have drug resistance to oseltamivir; that maybe an alert for treatment H1N1 influenza.

In N1, N2, and N7 pharmacophore comparison analysis, we brought up a proposal for design the versatile inhibitor of N1, N2, and N7 by combining ligand-based pharmacophore map and protein interaction maps. The ligand-based pharmacophore map was created from Lu's study (Lu *et al.*, 2008). Additionally, the map was consists with Shie's study (Shie *et al.*, 2008). Accordingly, the result was reliable. The protein-based pharmacophore maps were constructed by the protein structures of N2 and N7, using the protocol of interaction generation. By the protocol of pharmacophore comparison, the RMSD values between the three kinds of NA were calculated, then, the most matched map was elevated from the three maps. The most matched map was refined to form the combined map. The combined map fit Russell's report (Russell *et al.*, 2006). Based

on this reason, the map was employed to virtual screening on NCI database. The screening results were analyzed by the ligandfit docking program. Six compounds were suggested as potent versatile inhibitors by their fit values and docking scores (Figure 16). We hope to put forward a constructive conception of designing H1N1 inhibitors.

5. 參考文獻(References)

Bersuker, I.B., S. Bahceci, and J.E. Boggs, “Improved electron-conformational method of pharmacophore identification and bioactivity prediction. Application to angiotensin converting enzyme inhibitors,” *J. Chem. Inf. Comput. Sci.* 40, 1363 (2000).

Chen, C. Y. C, “Discovery of novel inhibitors for c-Met by virtual screening and pharmacophore analysis,” *J. Chin. Inst. Chem. Eng.* 39, 617 (2008a).

Chen, C. Y. C, “Inhibiting the vascular smooth muscle cells proliferation by EPC and DPPC liposomes encapsulated magnolol,” *J. Chin. Inst. Chem. Eng.* 39, 407 (2008b).

Chen, C. Y. C. "Insights into the suanzaoren mechanism-From constructing the 3D structure of GABA-A receptor to its binding interaction analysis." *J. Chin. Inst. Chem. Eng.* 39, 663 (2008c).

Chen, C. Y. C, “A novel perspective on designing the inhibitor of HER2 receptor,” *J. Chin. Inst. Chem. Eng.* 39, 291 (2008d).

Chen, C. Y. C, "Chemoinformatics and pharmacoinformatics approach for exploring the GABA-A agonist from Chinese herb suanzaoren," *J. Chin. Inst. Chem. Eng.* 40, 36 (2009a).

Chen, C. Y. C, "De novo design of novel selective COX-2 inhibitors: From virtual screening to pharmacophore analysis," *J. Chin. Inst. Chem. Eng.* 40, 55 (2009b).

Chen, C. Y. C, "Pharmacoinformatics approach for mPGES-1 in anti-inflammation by 3D-QSAR pharmacophore mapping," *J. Chin. Inst. Chem. Eng.* 40, 155 (2009c).

Cheung, C. Y., L. L. Poon, A. S. Lau, W. Luk, Y. L. Lau, K. F. Shortridge, S. Gordon, Y. Guan, and J. S. Peiris, "Induction of proinflammatory cytokines in human macrophages by influenza A (H5N1) viruses: a mechanism for the unusual severity of human disease?" *Lancet* 360, 1831 (2002).

Collins, P. J., L. F. Haire, Y. P. Lin, J. Liu, R. J. Russell, P. A. Walker, J. J. Skehel, S. R. Martin, A. J. Hay, and S. J. Gamblin, "Crystal structures of oseltamivir-resistant influenza virus neuraminidase mutants," *Nature* 453, 1258 (2008).

Gehlhaar, D. K., D. Bouzida, P. A. Rejto, "*Rational Drug Design: Novel Methodology and Practical Applications* ; Parrill, L.; Rami Reddy, M; Series title: ACS symposium series," *American Chemical Society* 719, 292 (1999).

Gehlhaar, D. K., G. M. Verkhivker, P. A. Rejto, C. J. Sherman, D. B. Fogel, L. J. Fogel, S. T. Freer, "Molecular Recognition of the Inhibitor AG-1343 by HIV-1 Protease: Conformationally Flexible Docking by Evolutionary Programming," *Chemistry & Biology* 2, 317 (1995).

Hauge, S. H., S. Dudman, K. Borgen, A. Lackenby, and O. Hungnes, "Oseltamivir-resistant influenza viruses A (H1N1), Norway, 2007-08," *Emerg. Infect. Dis.* 15, 155 (2009).

Ho, H. T., A. C. Hurt, J. Mosse, and I. Barr, "Neuraminidase inhibitor drug susceptibility differs between influenza N1 and N2 neuraminidase following mutagenesis of two conserved residues," *Antiviral. Res.* 76, 263 (2007).

Kash, J. C., T. M. Tumpey, S. C. Proll, V. Carter, O. Perwitasari, M. J. Thomas, C. F. Basler, P. Palese, J. K. Taubenberger, A. Garcia-Sastre, D. E. Swayne, and M. G. Katze, "Genomic analysis

of increased host immune and cell death responses induced by 1918 influenza virus," *Nature* 443, 578 (2006).

Kobasa, D., S. M. Jones, K. Shinya, J. C. Kash, J. Copps, H. Ebihara, Y. Hatta, J. H. Kim, P. Halfmann, M. Hatta, F. Feldmann, J. B. Alimonti, L. Fernando, Y. Li, M. G. Katze, H. Feldmann, and Y. Kawaoka, "Aberrant innate immune response in lethal infection of macaques with the 1918 influenza virus," *Nature* 445, 319 (2007).

Kurogi, Y. and O.F. Guner, "Pharmacophore modeling and three-dimensional database searching for drug design using catalyst," *Curr. Med. Chem.* 8, 1035 (2001).

Kurogi, Y., K. Miyata, T. Okamura, K. Hashimoto, K. Tsutsumi, M. Nasu, and M. Moriyasu, "Discovery of novel mesangial cell proliferation inhibitors using a three-dimensional database searching method," *J. Med. Chem.* 44, 2304 (2001).

Lu, W.J., Y.L. Chen, W.P. Ma, X.Y. Zhang, F. Luan, M.C. Liu, X.G. Chen, and Z.D. Hu, "QSAR study of neuraminidase inhibitors based on heuristic method and radial basis function network," *Eur. J. Med. Chem.* 43, 569 (2008).

Moscona, A, "Global transmission of oseltamivir-resistant influenza," *N. Engl. J. Med.* 360, 953 (2009).

Muegge, I. and Y. C. Martin, "A General and Fast Scoring Function for Protein-Ligand Interactions: A Simplified Potential Approach," *J. Med. Chem.* 42, 791 (1999).

Mukhtar, M. M., S. T. Rasool, D. Song, C. Zhu, Q. Hao, Y. Zhu, and J. Wu, "Origin of highly pathogenic H5N1 avian influenza virus in China and genetic characterization of donor and recipient viruses," *J. Gen. Virol.* 88, 3094 (2007).

Palese, P, "Influenza: old and new threats," *Nat. Med.* 10, S82 (2004).

Raymond, L. W. and L. Leach, "Treatment of post-influenza pneumonia in health care workers," *J. Occup. Environ. Med.* 49, 1181 (2007).

Russell, R. J., L. F. Haire, D. J. Stevens, P. J. Collins, Y. P. Lin, G. M. Blackburn, A. J. Hay, S. J. Gamblin, and J. J. Skehel, "The structure of H5N1 avian influenza neuraminidase suggests new opportunities for drug design," *Nature* 443, 45 (2006).

Shie J. J., J. M, Fang, C.H. Wong, "A concise and flexible synthesis of the potent anti-influenza agents tamiflu and tamiphosphor," *Angew. Chem. Int. Ed. Engl.* 47, 5788 (2008).

Shimbo, T., M. Kawachi, K. Saga, H. Fujita, T. Yamazaki, K. Tamai, and Y. Kaneda, "Development of a transferrin receptor-targeting HVJ-E vector," *Biochem. Biophys. Res. Commun.* 364, 423 (2007).

Shirvan, A. N., M. Moradi, M. Aminian, and R. Madani, "Preparation of neuraminidase-specific antiserum from the H9N2 subtype of avian influenza virus," *Turk. J. Vet. Anim. Sci.* 31, 219 (2007).

Stevens, J., A. L. Corper, C.F. Basler, J. K. Taubenberger, P. Palese, I. A. Wilson, "Structure of the uncleaved human H1 hemagglutinin from the extinct 1918 influenza virus," *Science* 303, 1866, (2004).

Takabatake, N., M. Okamura, N. Yokoyama, K. Okubo, Y. Ikehara, and I. Igarashi, "Involvement of a host erythrocyte sialic acid content in Babesia bovis infection," *J. Vet. Med. Sci.* 69, 999 (2007).

Teramoto, R., and H. Fukunishi, "Consensus Scoring with Feature Selection for Structure-Based Virtual Screening" *J. Chem. Inf. Model.* 48, 288 (2008).

Table 1. The structures of 18 compounds in data set.

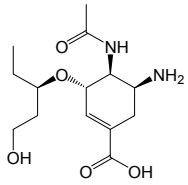	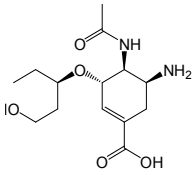	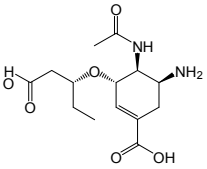	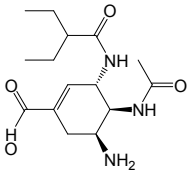	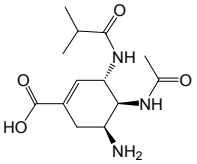
01	02	03	04	05
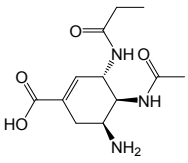	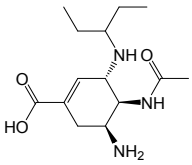	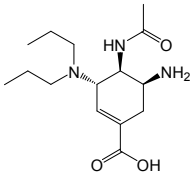	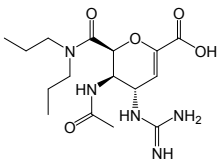	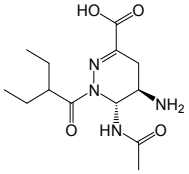
06	07	08	09	10
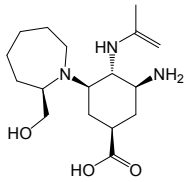	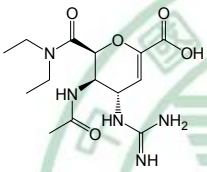	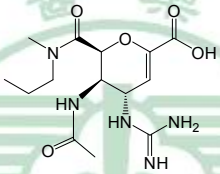	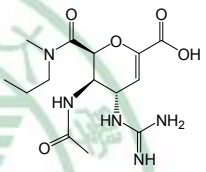	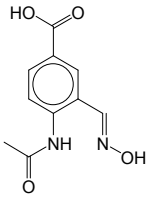
11	12	13	14	15
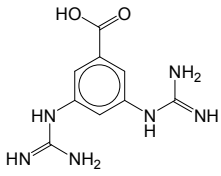	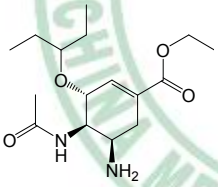	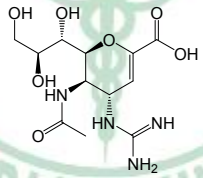		
16	oseltamivir	zanamivir		

Table 2. The 18 compounds of data set.

Name	Activ	Uncert	Principal	MaxOmitFeat
01	40	3.0	2	0
02	30	3.0	2	0
03	6	3.0	2	0
04	4000	3.0	0	0
05	6400	3.0	0	0
06	2700	3.0	0	0
07	11	3.0	2	0
08	12	3.0	2	0
09	6	3.0	2	0
10	6000	3.0	0	0
11	8	3.0	2	0
12	0.001	3.0	2	0
13	0.004	3.0	2	0
14	0.002	3.0	2	0
15	5500.47	3.0	0	0
16	1500.03	3.0	0	0
oseltamivir	0.001	3.0	2	0
zanamivir	0.005	3.0	2	0

Activ: It represented the compounds' tested activities, which must be greater than 0.0.

Uncert: It represented the ratio range of uncertainty in the activity value, set to 3.0 by default.

Principal: It indicates whether the ligand was active (Principal= 2) or inactive (Principal= 0).

MaxOmitFeat: It indicates how many features are allowed to miss for each molecule. By default, MaxOmitFeat was set to 0.

Table 3. Interaction types of PLP1

	Receptor PLP type			
Ligand PLP type	**Donor**	**Acceptor**	**Both**	**Non-polar**
Donor	Steric	H-bond	H-bond	Steric
Acceptor	H-bond	Steric	H-bond	Steric
Both	H-bond	H-bond	H-bond	Steric
Non-polar	Steric	Steric	Steric	Steric

This table is obtained from Gehlhaar's study (Gehlhaar *et al.*, 1995; Gehlhaar *et al.*, 1999).

Table 4. Parameters for PLP1 functional form

Interaction type	A	B	C	D	E	F
H-bond	2.3	2.6	3.1	3.4	-2.0	20.0
Steric	3.4	3.6	4.5	5.5	-0.4	20.0

This data is obtained from Gehlhaar's study (Gehlhaar *et al.*, 1995; Gehlhaar *et al.*, 1999).

Table 5. Interaction types of PLP2

	Receptor PLP type			
Ligand PLP type	**Donor**	**Acceptor**	**Both**	**Non-polar**
Donor	Repulsion	H-bond	H-bond	Dispersion
Acceptor	H-bond	Repulsion	H-bond	Dispersion
Both	H-bond	H-bond	H-bond	Dispersion
Non-polar	Dispersion	Dispersion	Dispersion	Dispersion

This table is obtained from Gehlhaar's study (Gehlhaar *et al.*, 1995; Gehlhaar *et al.*, 1999).

Table 6. Parameters for PLP2 functional form

Interaction type	A	B	C	D	E	F
H-bond	2.3	2.6	3.1	3.4	-4.0	15.0
Dispersion	0.93σ	1.0σ	1.25σ	1.5σ	-0.4	15.0
Repulsion	3.2	6.0	-	-	1.5	1.5

This data is obtained from Gehlhaar's study (Gehlhaar *et al.*, 1995; Gehlhaar *et al.*, 1999).

Table 7. The results of hypotheses generation

Hypo No.	Total cost	Error	RMS	Correlation	Features
1	137.95	109.62	2.48	0.888	HBA,HBA,HBD,POS
2	147.84	116.57	2.64	0.873	HBA,HBA,HBD,POS
3	148.04	118.88	2.69	0.867	HBA,HBA,HBA,POS
4	160.12	135.89	3.04	0.822	HBA,HBA,HBD,POS
5	160.66	132.58	2.98	0.832	HBA,HBA,HBA,POS
6	160.66	125.63	2.84	0.854	HBA,HBA,HBA,POS
7	161.94	132.74	2.98	0.833	HBA,HBA,HBA,POS
8	162.67	137.30	3.07	0.819	HBA,HBA,HBA,POS
9	165.49	135.14	3.03	0.828	HBA,HBA,HBD,POS
10	165.59	133.63	2.99	0.832	HBA,HBA,HBA,POS

Null cost = 295.93, fixed cost = 69.68, configuration cost value = 11.375. HBA is hydrogen bond acceptor feature, HBD is hydrogen bond donor feature, and POS is positive ionizable feature.

Table 8. The screening results of NCI database by Hypogen.

Name	FitValue	Name	FitValue	Name	FitValue
NCI0007391	13.847	NCI0114058	12.833	NCI0054248	13.054
NCI0021560	13.847	NCI0127520	12.601	NCI0038478	13.052
NCI0026546	13.847	NCI0112522	12.584	NCI0004348	13.049
NCI0040756	13.847	NCI0119846	12.54	NCI0042714	13.043
NCI0052907	13.847	NCI0064452	12.434	NCI0040590	13.042
NCI0023881	13.764	NCI0118695	12.307	NCI0053257	13.024
NCI0005554	13.7	NCI0108578	12.113	NCI0040755	13.017
NCI0030926	13.598	NCI0158489	12.321	NCI0003099	13.007
NCI0042183	13.555	NCI0187635	12.233	NCI0019510	13.007
NCI0042186	13.554	NCI0187646	12.233	NCI0025275	13.002
NCI0053255	13.469	NCI0180972	12.144	NCI0052408	12.998
NCI0033688	13.435	NCI0608654	13.038	NCI0003100	12.996
NCI0054249	13.405	NCI0608643	13.036	NCI0040754	12.956
NCI0042132	13.372	NCI0608650	13.016	NCI0020273	12.949
NCI0021705	13.368	NCI0605741	13.015	NCI0025286	12.929
NCI0058600	13.349	NCI0608647	12.991	NCI0023116	12.925
NCI0050744	13.326	NCI0605737	12.979	NCI0020670	12.9
NCI0058602	13.323	NCI0607157	12.978	NCI0024998	12.86
NCI0034519	13.293	NCI0607158	12.956	NCI0047648	12.855
NCI0051425	13.291	NCI0521703	12.789	NCI0019772	12.853
NCI0051448	13.288	NCI0521704	12.789	NCI0021557	12.853
NCI0040589	13.267	NCI0345087	12.257	NCI0023900	12.853
NCI0044443	13.262	NCI0606258	12.247	NCI0020275	12.846
NCI0025270	13.26	NCI0604985	12.209	NCI0000758	12.84
NCI0046331	13.197	NCI0604166	12.134	NCI0037779	12.84
NCI0051447	13.179	NCI0275619	12.028	NCI0020270	12.814
NCI0035900	13.178	NCI0353858	12.028	NCI0040705	12.811
NCI0042330	13.178	comp45	13.318	NCI0022699	12.799
NCI0049809	13.178	XW-630	12.307	NCI0020271	12.77
NCI0014083	13.132	NCI0020261	12.216	NCI0009698	12.73
NCI0018702	13.118	NCI0036875	12.202	NCI0016531	12.714
NCI0018712	13.118	NCI0044277	12.193	NCI0025020	12.552
NCI0022941	13.118	NCI0055554	12.192	NCI0018343	12.549
NCI0022942	13.118	NCI0055555	12.192	NCI0024533	12.549

NCI0058595	12.252	NCI0055560	12.192	NCI0033298	12.549
NCI0047461	12.245	NCI0055561	12.192	NCI0009629	12.542
NCI0056714	12.245	NCI0007290	12.17	NCI0025962	12.523
NCI0057034	12.245	NCI0051451	12.149	NCI0047151	12.516
NCI0043891	12.244	NCI0013252	12.108	NCI0040586	12.515
NCI0050352	12.244	NCI0044180	12.108	NCI0039358	12.509
NCI0056711	12.244	NCI0018757	12.026	NCI0018695	12.507
NCI0009130	12.237	NCI0044283	12.009	NCI0025274	12.501
NCI0044181	12.237	NCI0051812	12.287	NCI0043417	12.484
NCI0056275	12.345	NCI0003055	12.283	NCI0029431	12.465
NCI0060439	12.31	NCI0048600	12.253	NCI0049798	12.443
NCI0014659	12.305	NCI0036314	12.35	NCI0015771	12.429
AC-983	13.176	NCI0624650	13.078	AC-984	13.134

Table 9. The screening results of NCI database by Hypogen (cont.).

Name	FitValue	Name	FitValue
PHOSPHATIDYLSERINE	12.334	DIBEKACIN	12.151
GP-1-515	12.327	PRADIMICIN-FL	12.125
GP-515	12.327	PENTETREOTIDE INDIUM	12.046
METHYL-OLIGOBIOSAMINIDE	12.302	CHAPSO	12.034
DIHYDROACARBOSE	12.267	VALIDOXYLAMINE-A	12.252
COLIMECYCLINE	12.225	TRESTATIN-A	12.049
STREPTOIMIDAZOLIDINE	12.219	ZYGACINE	12.048
PROTOVERINE	12.173	NCI0611895	13.035
APRAMYCIN	12.928	MANNOPEPTIMYCIN-DELTA	12.785
KANAMYCIN-C	12.339	MANNOPEPTIMYCIN-BETA	12.774
ACTINOSPECTINOIC-ACID	12.584	HYDROXYVALIDAMINE	12.77
BENANOMICIN-B	12.423	MANNOPEPTIMYCIN-GAMMA	12.751
4"-DEOXYTOBRAMYCIN	12.38	MANNOPEPTIMYCIN-EPSILON	12.742
NCI0645771	12.348	ETIMICIN	12.687
BEKANAMYCIN SULFATE	12.215	GENTAMICIN	12.687
NCI0685277	12.19	GENTAMYCIN-C1A	12.687
NCI0685281	12.19	DESMOSINE	12.654
NCI0632482	12.134	RKP-192	12.514
NCI0671266	12.095	LU-15-089	12.508
BB-K-89	12.011	LIPOSIDOMYCIN-C	12.425
SCH-21561	13.184	LIGA-20	12.412
RO-09-0766	13.026	SPHINGOSINE-PHOSPHATE-1	12.387
MANNOPEPTIMYCIN-ALPHA	12.837	IPX-750	12.883
APRAMYCIN SULFATE	12.928	DESTOMYCIN-A	12.366

Table 10. The docking results of the fifty compounds with H1.

Name	LigS1	LigS2	-PLP1	-PLP2	Jain	-PMF	-PMF04	DS	CS
DESTOMYCIN-A	4.72	4.35	46.64	46.71	0.35	67.82	20.32	47.29	8
NCI0624650	5.14	4.52	33.96	44.38	1.92	67.09	29.22	44.93	7
NCI0607158	4.32	4.03	39.37	33.30	-1.46	59.57	18.16	46.00	6
NCI0605741	4.56	4.33	46.85	46.78	2.36	41.36	7.12	43.15	6
NCI0608647	4.94	4.20	31.56	31.19	-0.52	76.04	36.82	42.07	6
BB-K-89	3.96	4.24	45.99	45.78	-0.80	57.22	12.29	41.90	6
PROTOVERINE	4.24	4.42	43.88	52.14	-0.29	34.51	-1.08	41.52	6
IPX-750	4.80	4.54	49.87	57.00	1.56	34.77	3.13	40.23	6
NCI0353858	4.21	3.49	21.40	26.58	0.35	69.00	39.62	64.60	5
NCI0605737	4.75	3.91	27.83	30.26	-0.41	74.57	39.51	44.73	5
GENTAMYCIN-A	4.15	4.36	40.58	39.27	-0.23	29.49	4.30	38.40	5
KANAMYCIN-C	4.19	4.60	52.82	57.44	0.26	34.32	12.73	38.02	5
NCI0685277	4.43	4.29	41.48	44.62	1.00	28.83	-1.88	37.69	5
NCI0685281	4.43	4.29	41.48	44.62	1.00	28.83	-1.88	37.69	5
APRAMYCIN	5.01	4.64	66.28	67.52	1.05	30.64	1.82	31.62	5
NCI0608643	4.07	4.41	36.85	35.90	-1.96	27.31	1.35	41.15	4
NCI0606258	3.39	4.19	35.53	33.49	-1.69	61.99	18.05	41.09	4
NCI0608650	4.12	3.62	24.44	24.57	-1.43	65.67	34.59	39.85	4
GP-1-515	4.26	4.00	30.92	29.08	-0.26	30.53	7.32	38.81	4
GP-515	4.26	4.00	30.92	29.08	-0.26	30.53	7.32	38.81	4
NCI0671266	4.13	3.36	23.89	27.73	-0.66	85.59	44.36	38.81	4
4"-DEOXYTOBRAMYCIN	4.63	4.42	33.02	33.74	-1.79	79.24	38.29	33.01	4
SPHINGOSINE-PHOSPHATE-1	4.06	4.27	44.73	44.77	-1.52	51.41	11.03	25.87	4
DIHYDROACARBOSE	5.24	4.55	48.60	52.66	-2.66	22.15	-1.27	6.86	4
Zanamivir	4.34	3.80	29.32	31.90	-1.08	85.92	37.05	45.00	4
NCI0611895	3.59	3.99	21.88	18.33	-2.57	59.60	28.34	42.46	3
NCI0607157	4.05	3.79	39.61	37.31	-1.63	31.77	5.06	41.12	3
ACTINOSPECTINOIC-ACID	2.91	3.15	10.84	15.82	-2.45	49.60	19.44	38.84	3
PHOSPHATIDYLSERINE	3.48	3.51	16.75	13.26	-0.37	50.90	23.99	32.84	3
NCI0275619	2.88	3.50	23.40	26.12	0.60	53.55	26.13	32.71	3
ETIMICIN	1.10	3.86	38.96	37.94	-1.32	47.11	11.55	31.51	3
GENTAMICIN	1.10	3.86	38.96	37.94	-1.32	47.11	11.55	31.51	3
GENTAMYCIN-C1A	1.10	3.86	38.96	37.94	-1.32	47.11	11.55	31.51	3
BENANOMICIN-B	2.94	4.03	48.00	41.39	-3.23	33.47	2.83	30.71	3
NCI0608654	2.56	3.24	26.48	27.34	-1.30	42.56	21.02	41.98	2

METHYL-OLIGOBIOSAMINIDE	3.12	3.33	27.05	34.86	-1.21	44.88	25.47	38.43	2
DIBEKACIN	2.55	3.20	21.82	20.73	-3.97	52.53	15.62	35.29	2
HYDROXYVALIDAMINE	3.18	3.12	13.78	16.33	-1.14	52.67	26.77	33.87	2
Oseltamivir	3.05	3.99	50.47	46.67	-0.88	-6.35	-30.19	23.90	2
NCI0158489	4.06	3.90	29.95	34.48	-1.29	37.31	13.05	39.63	1
NCI0345087	3.10	3.41	26.09	29.65	-1.64	37.33	13.89	24.72	1
NCI0521703	2.01	3.79	25.97	23.76	-0.76	26.03	-12.23	24.67	1
NCI0521704	2.01	3.79	25.97	23.76	-0.76	26.03	-12.23	24.67	1
SCH-21561	1.11	2.86	13.83	12.37	-4.14	40.90	17.74	24.23	1
PRADIMICIN-FL	3.55	3.98	37.29	33.07	-5.95	40.70	8.46	14.06	1
DESMOSINE	1.75	3.38	35.05	27.79	-4.73	17.63	-1.30	34.04	0
NCI0187635	-6.82	-11.83	-23.22	-12.94	-2.91	38.35	6.38	26.00	0
NCI0187646	-6.82	-11.83	-23.22	-12.94	-2.91	38.35	6.38	26.00	0
LU-15-089	1.12	3.35	35.11	33.51	-2.38	-9.65	-9.14	25.60	0
STREPTOIMIDAZOLIDINE	1.46	2.87	15.22	13.37	-6.45	39.55	11.67	24.47	0

DS : docking score; CS : consensus score.

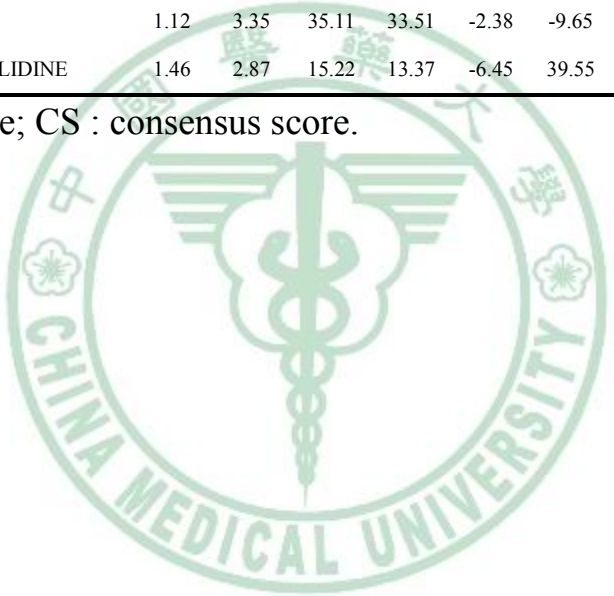

Table 11. The docking results of the forty-six compounds with N1.

Name	LigS1	LigS2	-PLP1	-PLP2	Jain	-PMF	-PMF04	DS	CS
KANAMYCIN-C	6.94	6.92	93.83	105.07	6.43	230.59	165.70	72.23	8
PROTOVERINE	6.94	6.14	71.04	84.73	4.19	244.60	130.43	81.01	8
Zanamivir	5.68	5.73	72.21	77.73	1.49	200.16	123.85	78.41	8
NCI0624650	6.28	5.96	73.34	70.98	4.13	195.08	124.74	70.28	8
NCI0611895	6.86	6.97	69.55	75.67	5.62	195.20	136.36	76.18	8
APRAMYCIN	6.67	6.07	97.07	92.38	4.31	210.78	152.16	68.39	8
NCI0608654	6.81	6.41	74.08	79.23	5.06	191.55	125.29	68.81	8
NCI0608643	6.80	6.26	72.65	75.62	5.25	194.81	125.48	70.23	8
NCI0608650	6.61	5.96	66.67	73.31	4.26	185.81	121.62	74.41	8
NCI0605741	6.71	6.35	69.09	73.33	4.77	190.73	121.03	73.67	8
NCI0605737	6.60	6.05	67.56	75.32	5.15	188.56	118.85	71.18	8
NCI0607157	6.68	6.04	69.36	77.12	5.74	178.45	128.09	77.22	8
NCI0607158	6.78	6.23	73.52	80.63	5.21	204.98	135.52	83.52	8
NCI0606258	6.52	5.93	68.04	73.57	5.37	201.98	128.54	77.03	8
Oseltamivir	4.93	4.31	33.85	38.08	2.84	180.44	98.36	44.91	7
METHYL-OLIGOBIOSAMINIDE	6.30	5.92	68.37	79.88	2.42	190.64	131.79	71.41	7
DIBEKACIN	6.55	6.30	70.76	74.23	4.92	220.30	153.95	64.58	7
BENANOMICIN-B	7.54	5.88	104.70	101.44	4.78	216.61	139.35	19.84	7
NCI0671266	6.71	6.30	72.77	77.41	2.10	206.59	149.51	82.10	7
BB-K-89	7.15	6.46	97.05	76.41	5.38	179.67	127.28	59.88	7
NCI0158489	6.62	6.14	66.14	66.96	3.49	175.24	117.37	72.43	7
DESTOMYCIN-A	6.34	5.10	76.54	71.82	3.19	208.11	155.67	80.09	6
SCH-21561	5.53	4.92	72.56	78.35	6.08	204.71	135.57	35.61	5
LU-15-089	6.53	6.52	87.94	91.05	4.52	172.35	92.19	62.60	5
4"-DEOXYTOBRAMYCIN	6.09	6.00	69.01	65.97	2.51	185.19	131.35	56.64	5
NCI0685277	6.25	5.55	68.65	80.38	3.35	180.02	108.89	61.29	5
NCI0685281	6.25	5.55	68.65	80.38	3.35	180.02	108.89	61.29	5
NCI0608647	5.92	6.51	71.24	67.83	4.95	110.64	75.49	73.38	5
IPX-750	6.31	5.88	59.10	72.04	3.16	128.60	90.63	71.99	4
ETIMICIN	5.98	5.64	74.61	64.91	5.47	204.90	129.22	52.50	4
GENTAMICIN	5.98	5.64	74.61	64.91	5.47	204.90	129.22	52.50	4
GENTAMYCIN-C1A	5.98	5.64	74.61	64.91	5.47	204.90	129.22	52.50	4
DESMOSINE	6.93	5.94	78.44	83.02	1.73	171.65	115.90	45.11	4
GENTAMYCIN-A	6.79	5.26	71.71	64.17	2.03	218.87	159.36	60.45	4
ACTINOSPECTINOIC-ACID	6.49	5.96	64.50	65.78	2.46	217.50	139.58	63.91	4

NCI0345087	6.37	5.83	68.01	65.70	3.72	165.36	111.23	58.00	3
SPHINGOSINE-PHOSPHATE-1	5.91	4.95	63.62	73.98	-1.28	180.82	83.79	53.95	2
PHOSPHATIDYLSERINE	5.57	5.53	47.51	49.41	4.05	119.48	82.96	68.30	2
NCI0521703	5.37	6.01	46.60	46.86	4.40	116.76	95.14	57.74	2
NCI0521704	5.37	6.01	46.60	46.86	4.40	116.76	95.14	57.74	2
HYDROXYVALIDAMINE	5.41	5.77	58.93	60.98	4.48	104.51	67.53	58.55	1
NCI0275619	4.41	4.68	40.72	46.14	3.24	105.74	71.61	56.66	1
GP-1-515	5.27	4.82	34.81	28.74	-0.14	118.00	94.03	59.51	0
GP-515	5.27	4.82	34.81	28.74	-0.14	118.00	94.03	59.51	0
NCI0187635	3.96	4.82	49.58	37.41	1.12	124.82	79.27	53.53	0
NCI0187646	3.96	4.82	49.58	37.41	1.12	124.82	79.27	53.53	0

DS : docking score; CS : consensus score.

Table 12. Root-mean-squared error displacement (RMSD) in the results of comparison analysis.

N1	HBD	DonorPT1	HBA1	AcepterPT1	HBA2	AcepterPT2
N2	location1.416	location1.415	location1.168	location1.167	location1.182	location1.181
RMSD N1-N2	0.220	0.268	0.520	0.390	0.306	0.402
N7	location1.420	location1.419	location1.336	location1.335	location1.252	location1.251
RMSD N1-N7	0.300	0.280	0.543	0.604	0.298	0.553

Table 13. The top 6 potent versatile inhibitors from NCI database.

Name	dock score	Fit value
NCI0054249	129.058	13.405
NCI0040590	94.656	13.042
NCI0051451	83.849	12.149
NCI0040589	81.717	13.267
NCI0054248	81.579	13.054
VALIDOXYLAMINE-A	80.407	12.252

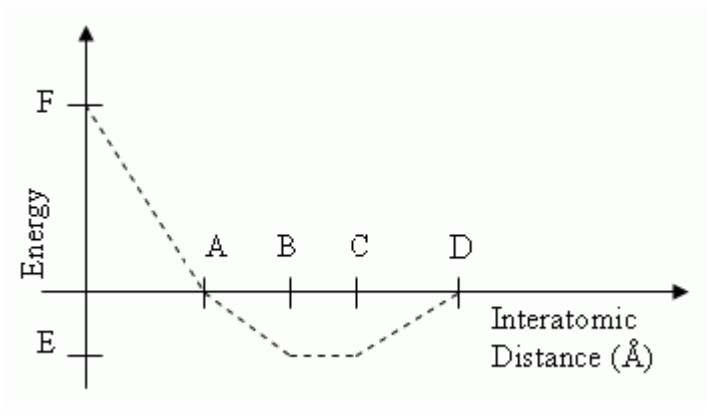

Figure 1. Functional form of PLP1. This figure is obtained from Gehlhaar's study (Gehlhaar *et al.*, 1995; Gehlhaar *et al.*, 1999).

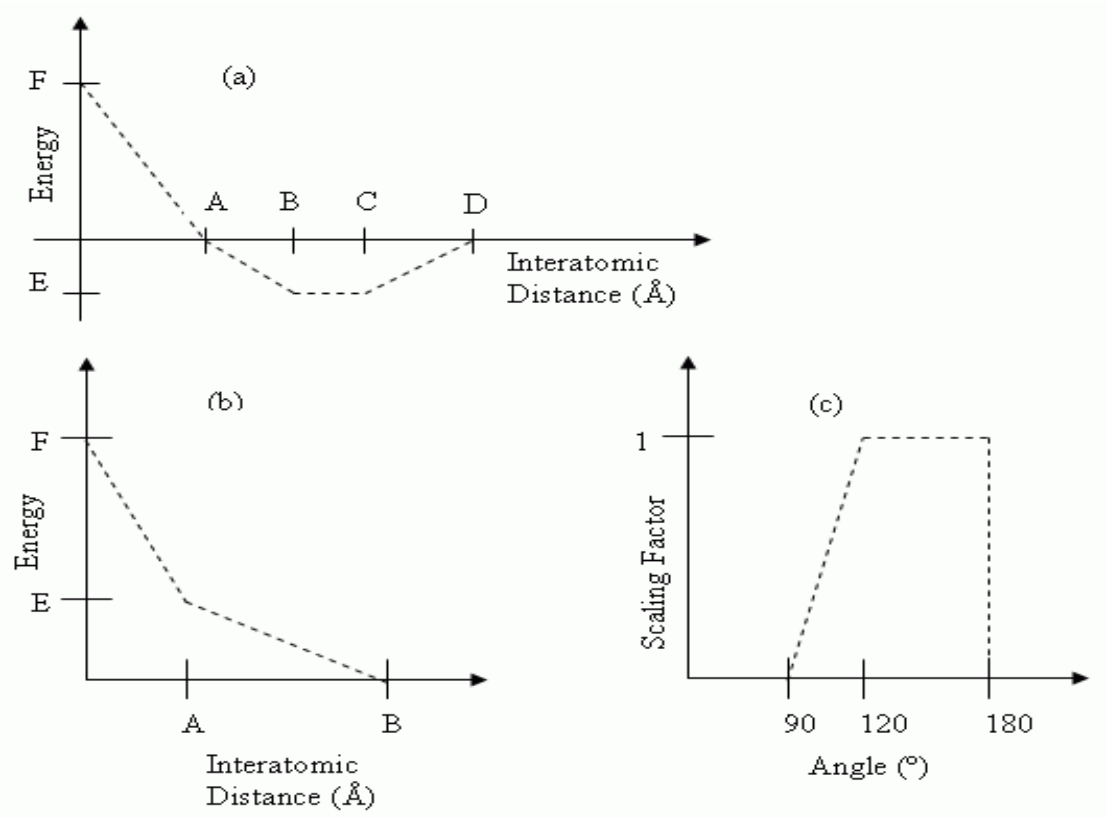

Figure 2. Functional forms of PLP2. (a) Pairwise potential for H-bond and dispersion terms. (b) Pairwise potential for repulsion terms. (c) Scaling factor for H-bond and repulsion terms based on the angle formed by the receptor and ligand atoms. This figure is obtained from Gehlhaar's study (Gehlhaar *et al.*, 1995; Gehlhaar *et al.*, 1999).

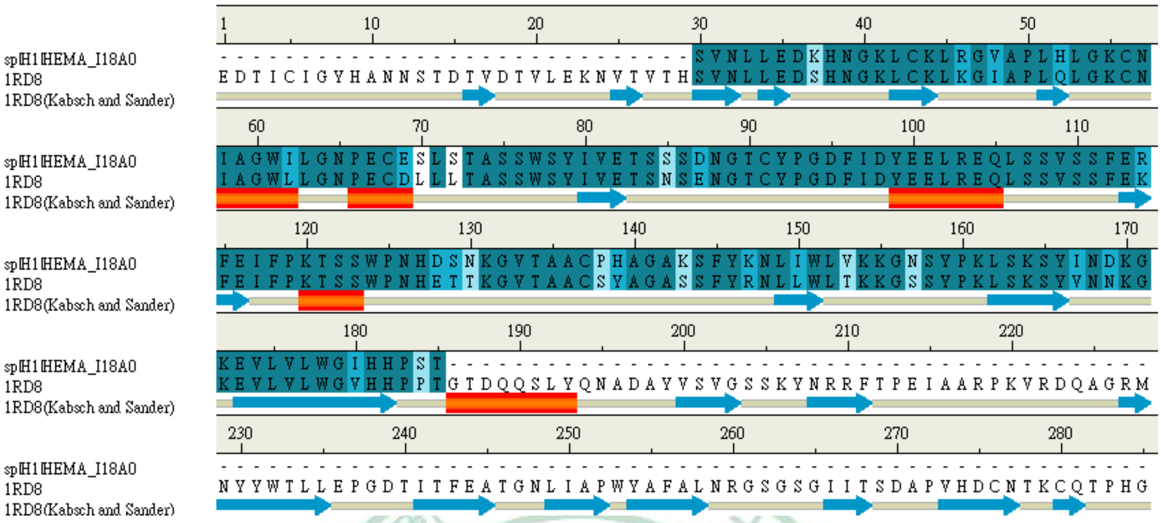

Figure 3. The result of H1 sequence alignment. The sequence identity and similarity between the latest H1 sequence and IRD8 are 70.8% and 78.9%, respectively.

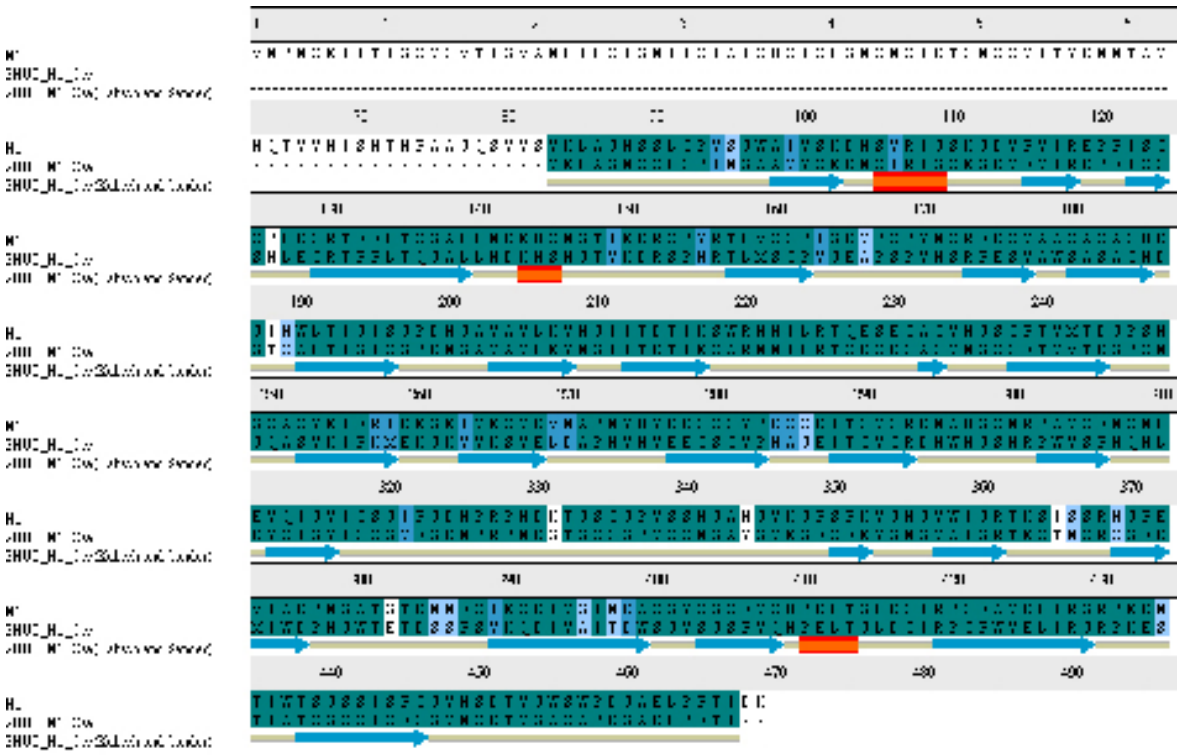

Figure 4. The results of N1 sequences alignment. The sequence identity and similarity between the latest N1 sequence and 2HU0 are 91.4% and 95.6%, respectively.

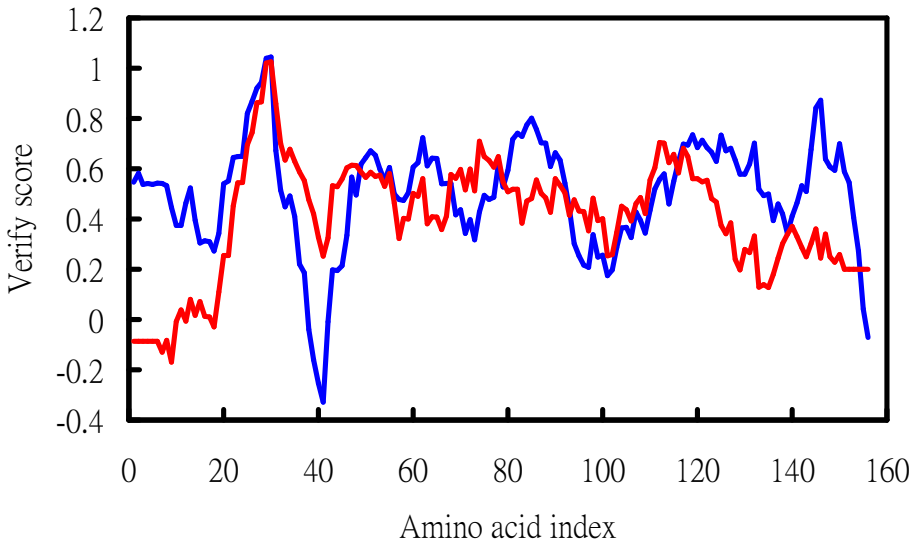

Figure 5. The results of verify score plot of H1 homology modeling. The red line is the latest H1 sequence and the blue line is the template (PDB ID: 1RD8) for modeling.

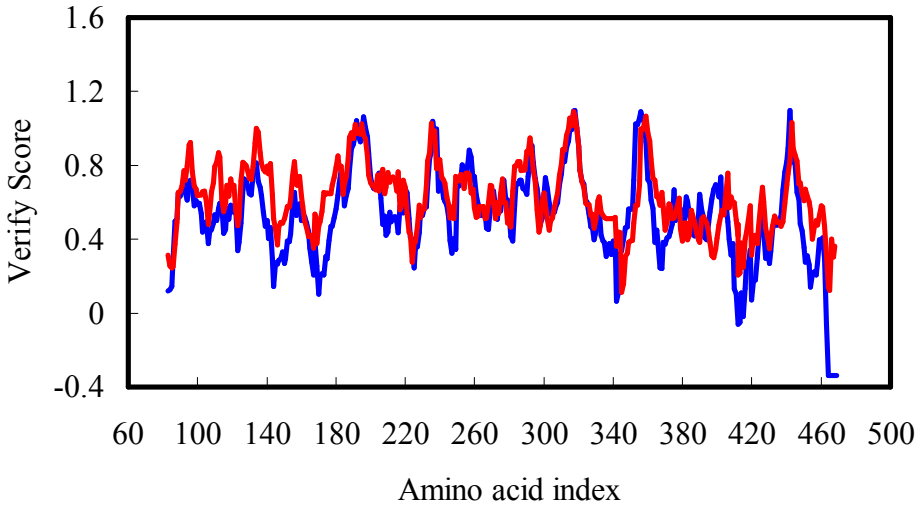

Figure 6. The results of verify score plot of N1 homology modeling. The Verify Score diagram shows the validity of our homology model. The amino acid from 119 to 293 is the major binding site. The blue line and the red line are the latest N1 sequence and the template (PDB ID: 2HU0), respectively.

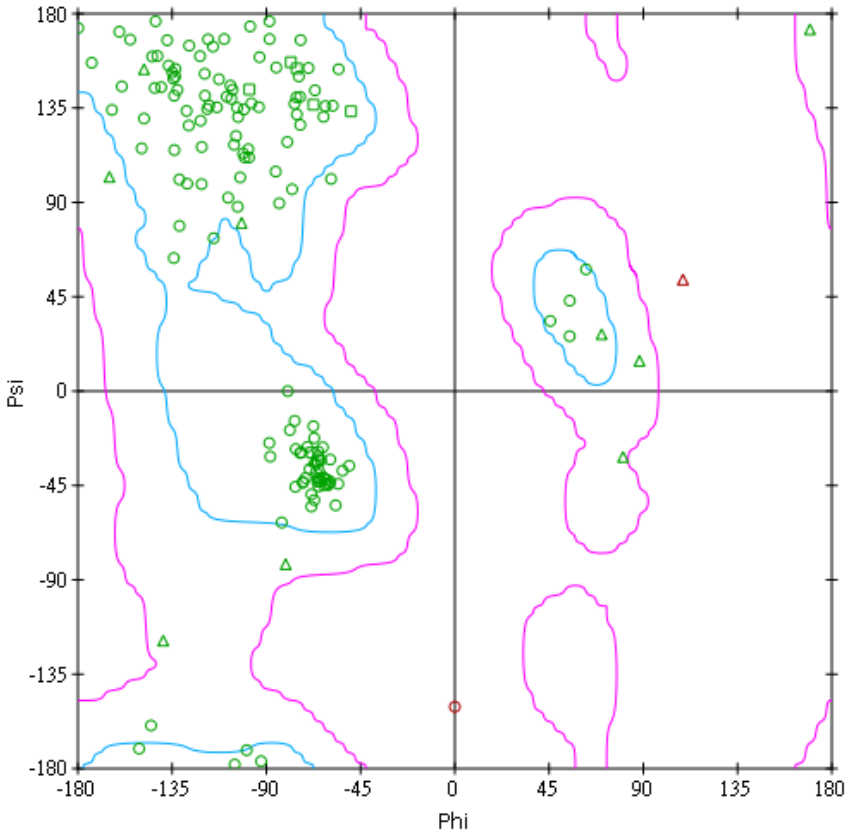

Figure 7. Ramachandran plotting of H1 homology modeling result. Glycine is labeled by triangles. It shows only 1.28% out of the region of possible angle formations.

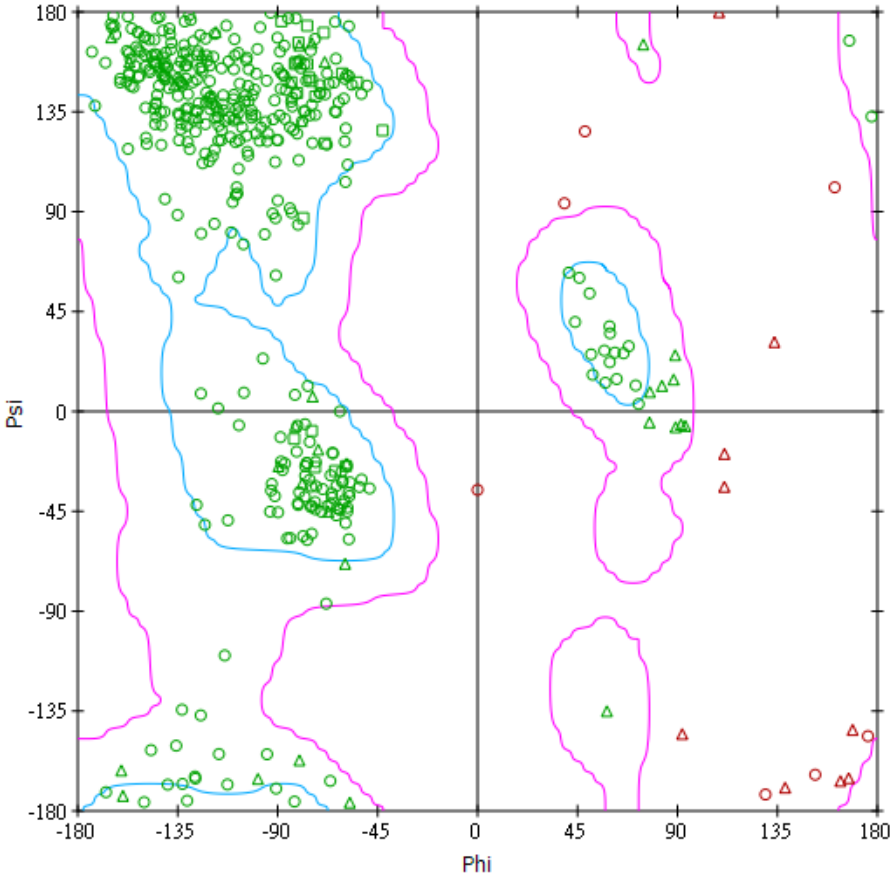

Figure 8. Ramachandran plotting of N1 homology modeling result. Glycine is labeled by triangles. It shows only 3.4% out of the region of possible angle formations.

(a)

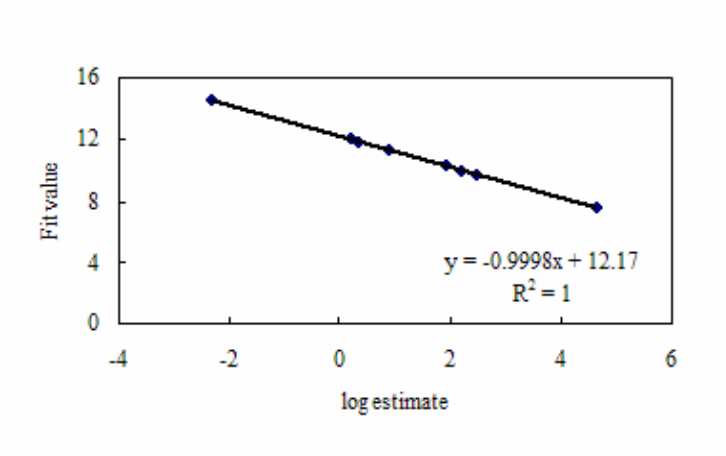

(b)

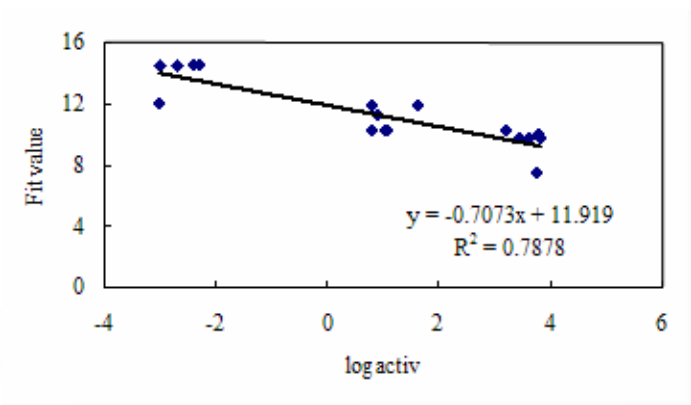

(c)

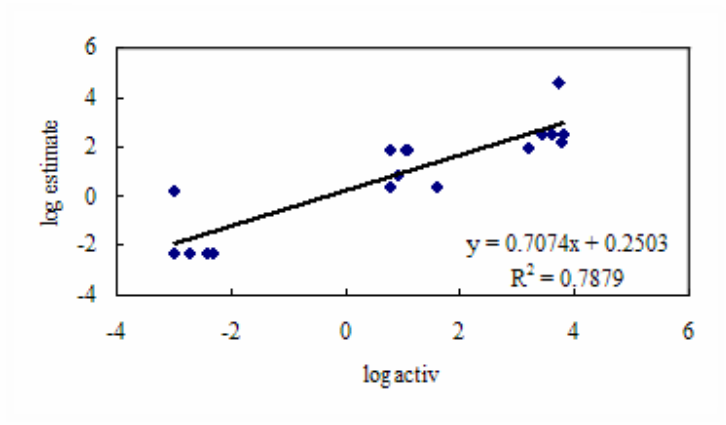

Figure. 9. The linear correlation of SAR. (a) The correlation of log estimate versus Fit value. (b)The plotting of Fit value versus log active. (c) The plotting of log estimates versus log active.

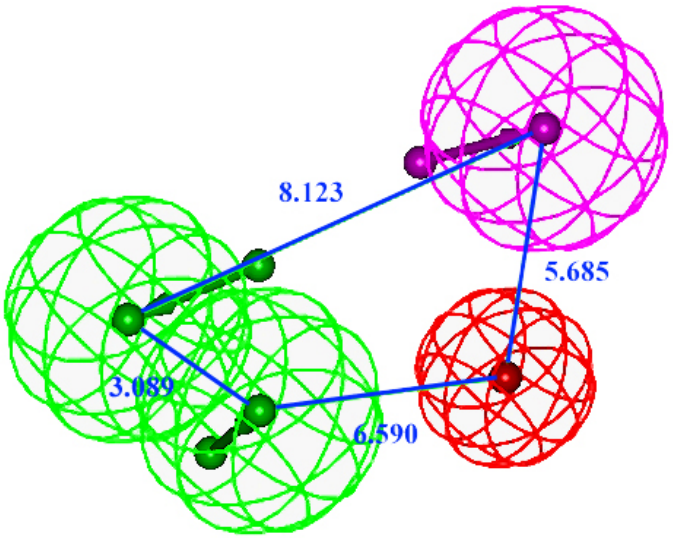

Figure 10. The features of hypotheses 1. The distances of features are labeled by blue lines. The green one is hydrogen bond acceptor feature, the purple one is hydrogen bond donor feature, and the red one is positive ionizable feature.

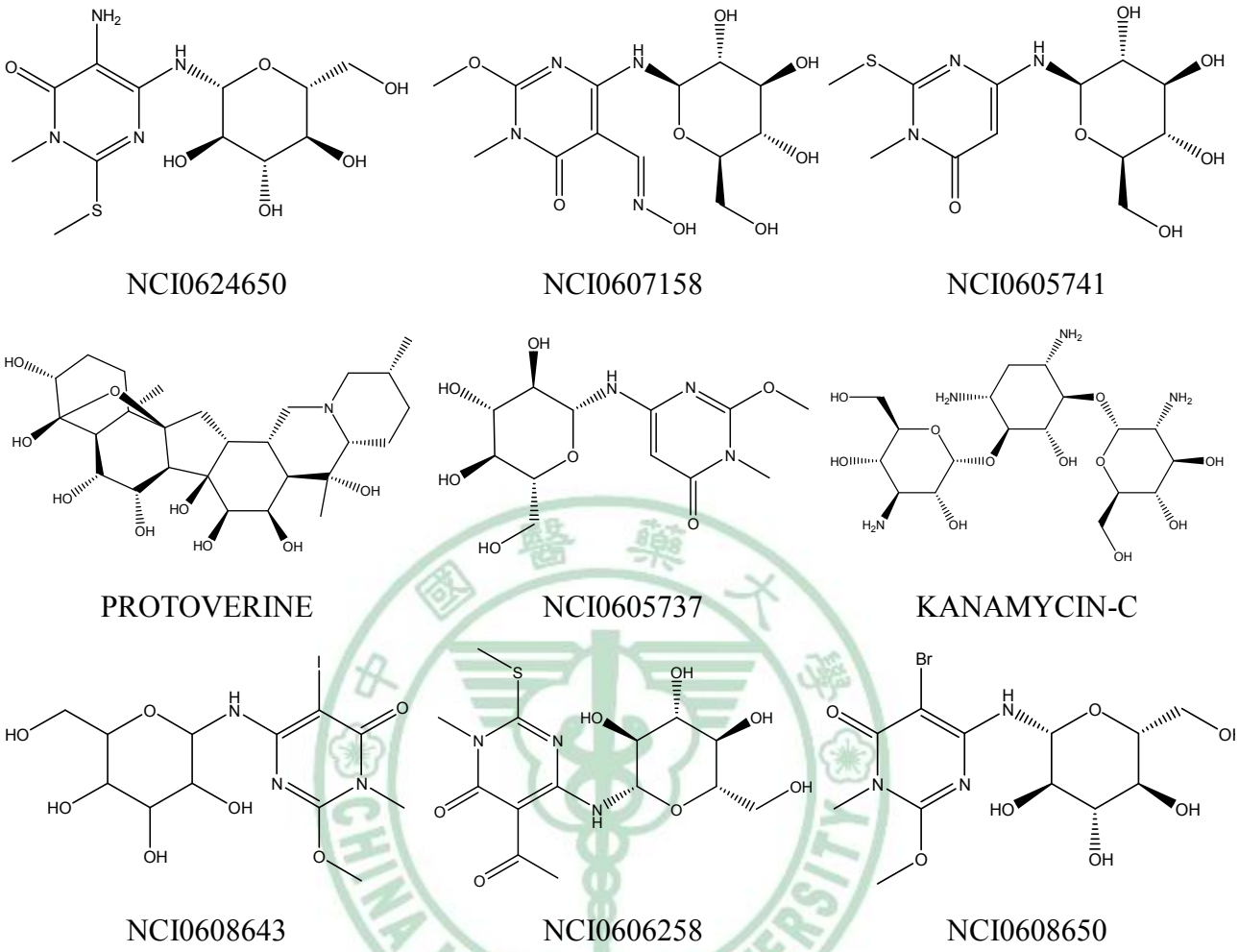

Figure 11. The chemical structures of top 9 candidates.

(a1)

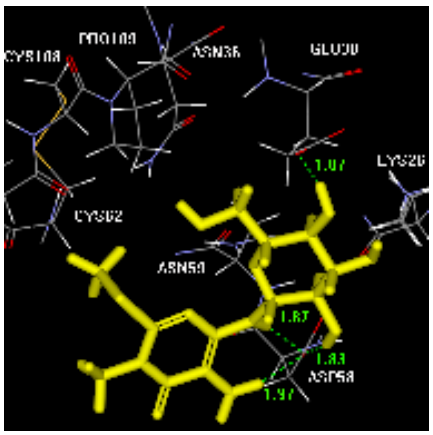

(a2)

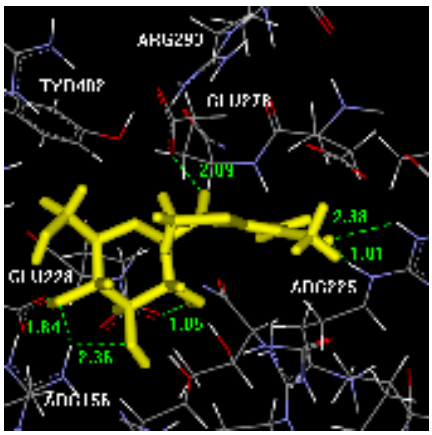

(b1)

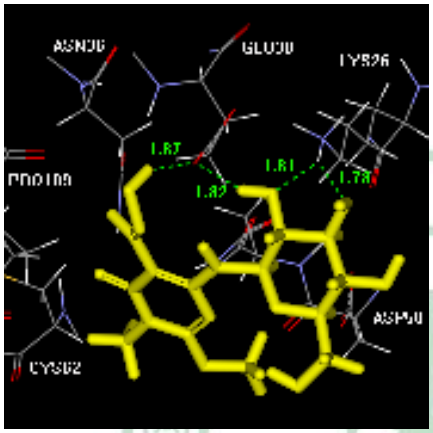

(b2)

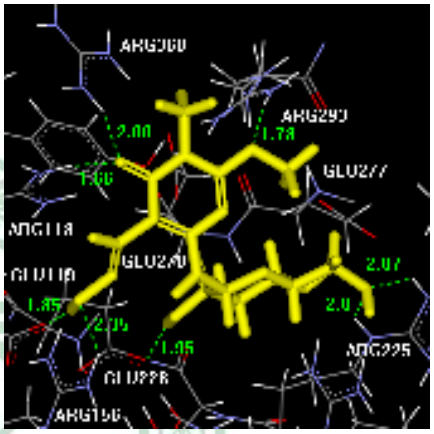

(c1)

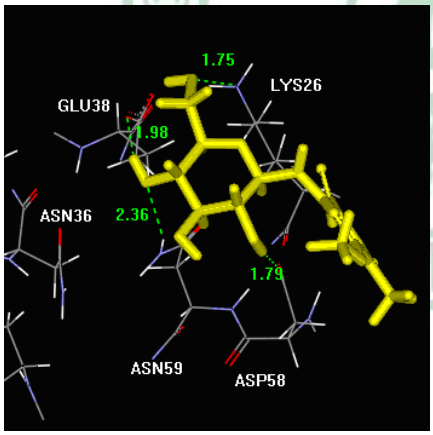

(c2)

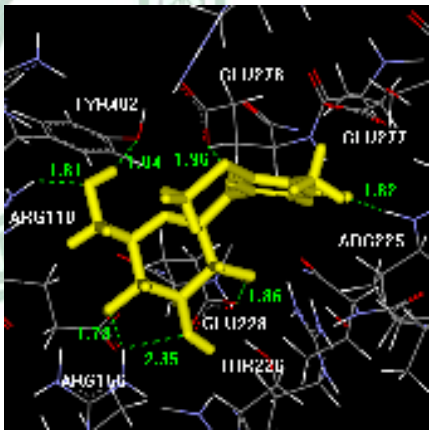

(d1)

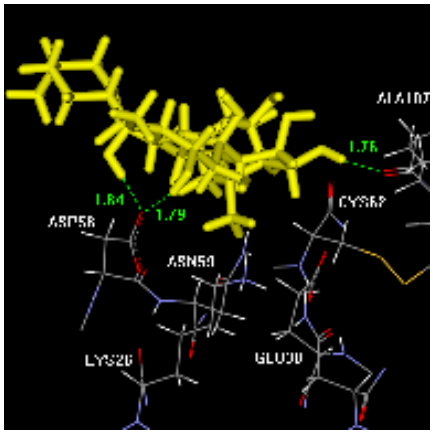

(d2)

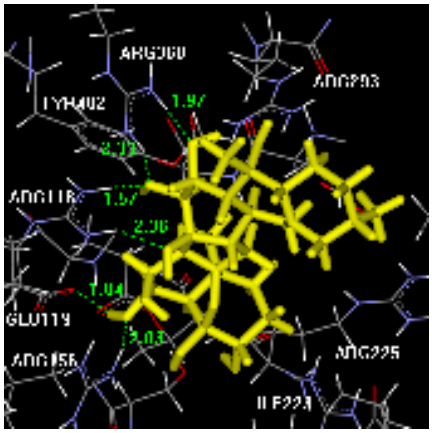

(e1)

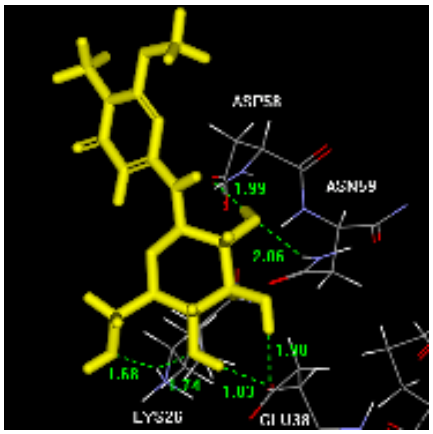

(e2)

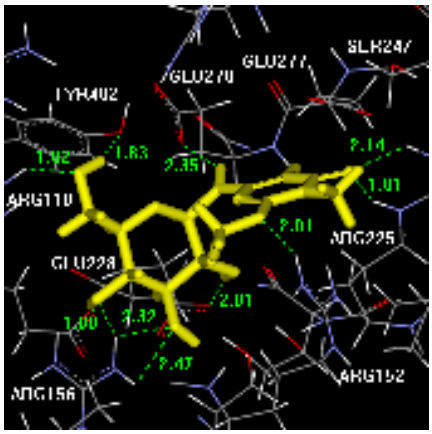

(f1)

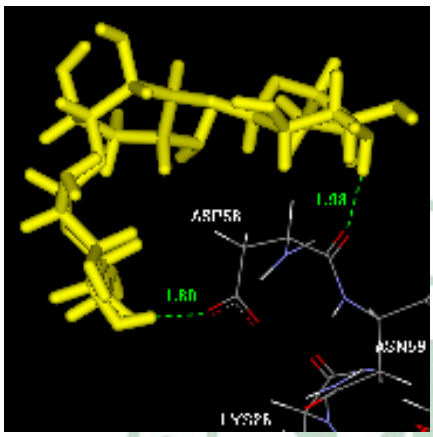

(f2)

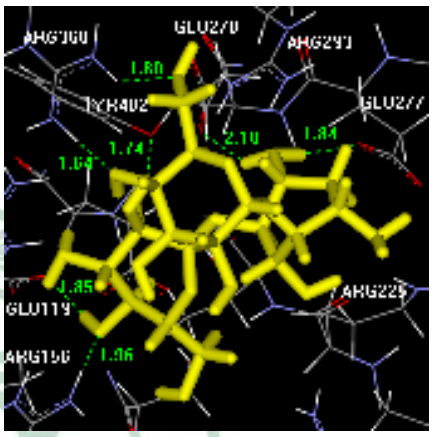

(g1)

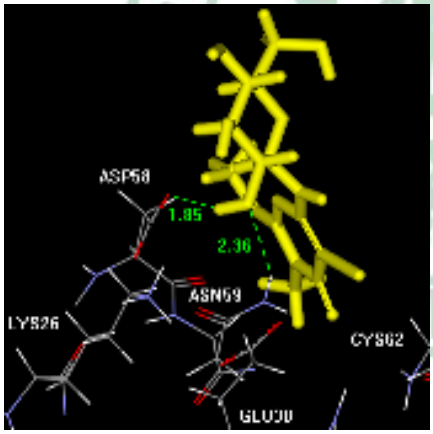

(g2)

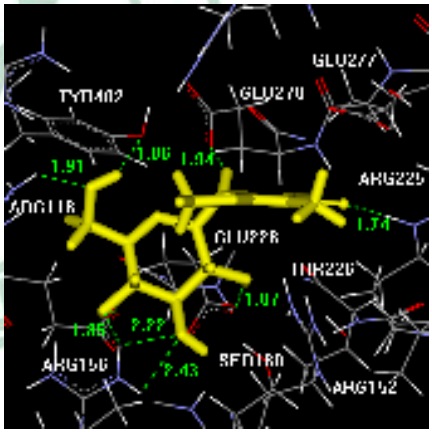

(h1)

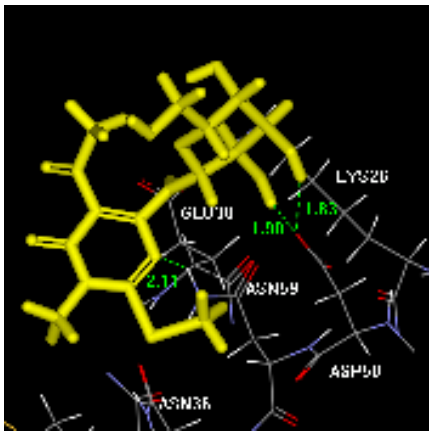

(h2)

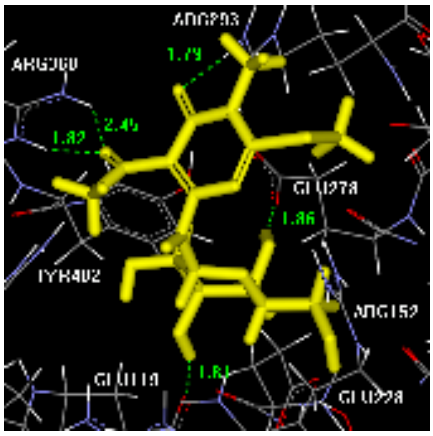

(i1) (i2)

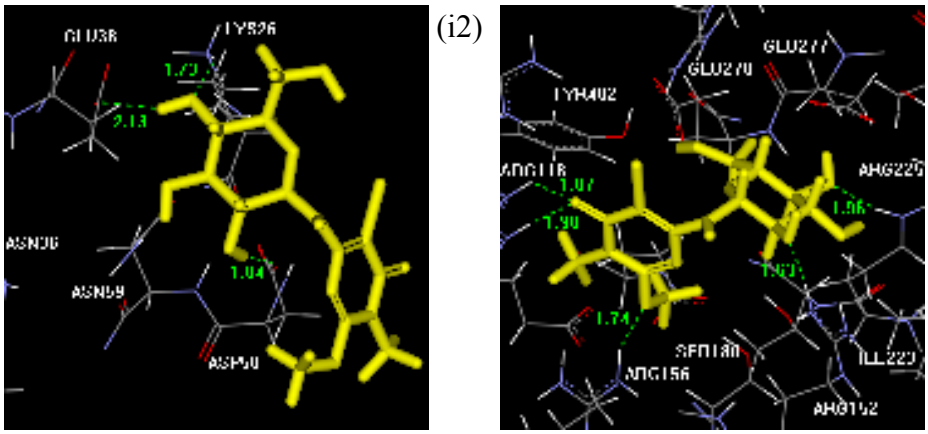

Figure 12. The docking poses of 9 candidates in H1 (a1-i1) and N1 (a2-i2), respectively. (a) NCI0624650, (b) NCI0607158, (c) NCI0605741, (d) PROTOVERINE, (e) NCI0605737, (f) KANAMYCIN-C, (g) NCI0608643, (h) NCI0606258, and (i) NCI0608650.

(a)

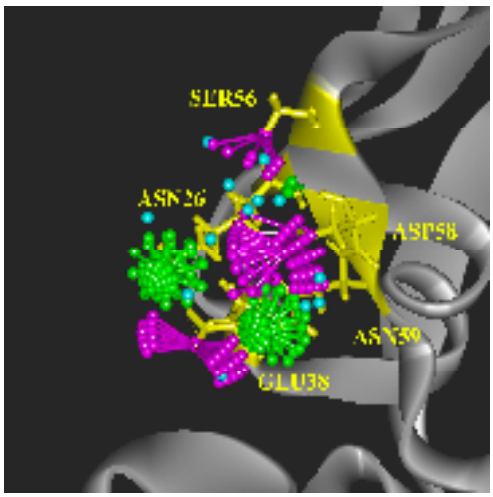

(b)

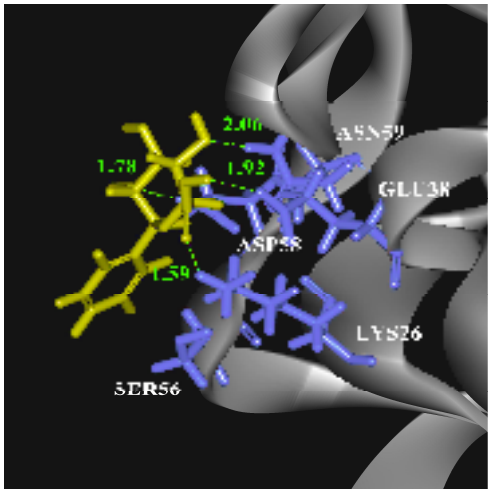

(c)

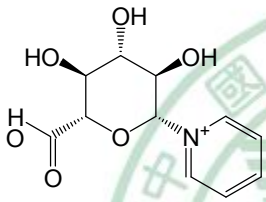

Figure 13. The pharmacophore analysis of H1. (a) The interaction map of the latest H1 structure. The green ones are hydrogen bond acceptor features; the purple ones are hydrogen bond donor features, and the blue ones are hydrophobic features. (b)The docking pose of NCI00353858 in H1. The hydrogen bonds are labeled by green dotted lines. (c) The structure of NCI0353858.

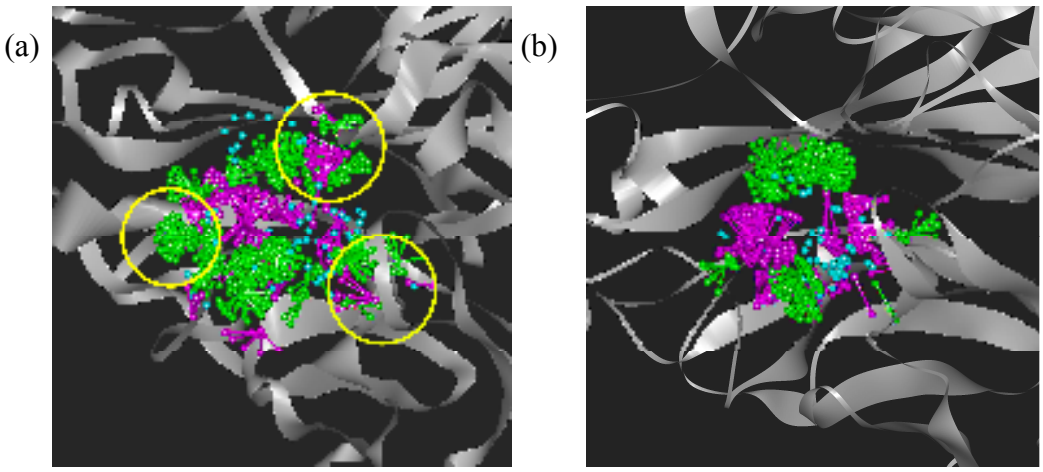

Figure 14. The interaction maps of N7 and N2. (a) The interaction map of N7. The green ones are hydrogen bond acceptor features, the purple ones are hydrogen bond donor features, and the blue ones are hydrophobic features. The yellow circles labeled the major differences between N2 and N7 interaction maps. (b)The interaction map of N2.

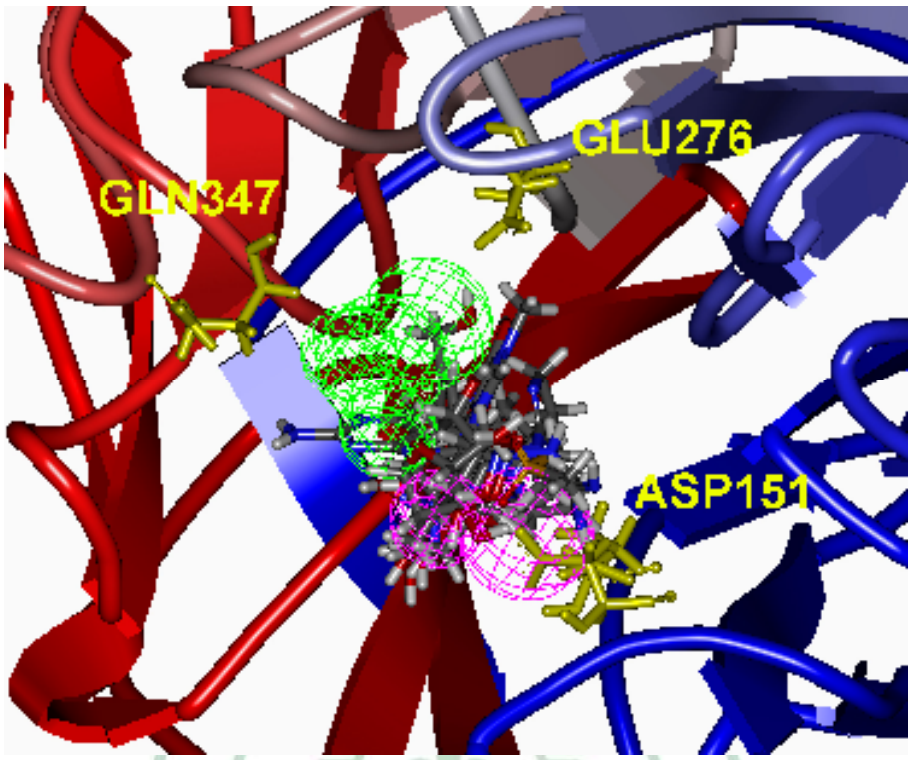

Figure 15. The combined map was fit in the binding site of N1. The top 6 potent compounds are showed in the binding site and fitted with the combined map.

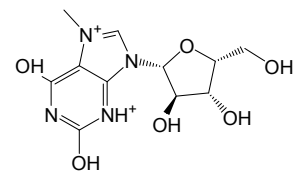

NCI0054249

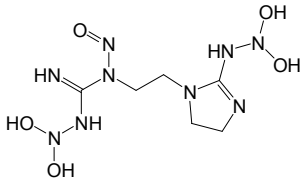

NCI0040590

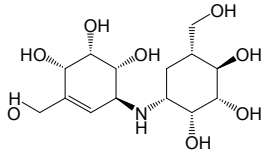

VALIDOXYLAMINE-A

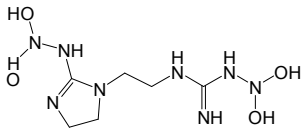

NCI0040589

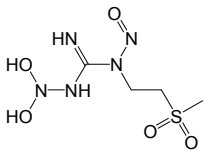

NCI0051451

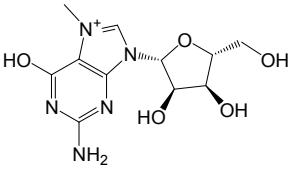

NCI0054248

Figure 16. The structures of the 6 candidates from NCI database.

6. 已發表之論文著作(Publications)

6-1. 論文發表 Journal publications

1. **Chien-yu Chen**、Yea-huey Chang、Da-Tian Bau、Hung-jin Huang、Fuu-Jen Tsai*、Chang-Hai Tsai*、Chen, Calvin Yu-Chian*，Discovery of potent inhibitors for phosphodiesterase 5 by virtual screening and pharmacophore analysis，ACTA PHARMACOLOGICA SINICA，2009 Nov
2. **Chien-Yu Chen**、Hung-Jin Huang、Fuu-Jen Tsai*、Chang-Hai Tsai*、Chen, Calvin Yu-Chian*，Development of AMP-activated protein kinase agonists by structure-based and ligand-based drug designing，ADVANCED MATERIALS & PROCESSES，2009 Oct
3. **Chien-Yu Chen**、Yea-Huey Chang、Fuu-Jen Tsai*、Chang-Hai Tsai*、Chen, Calvin Yu-Chian*，Fabrication of multi-functional SiO2@Au core-shell nanoparticles，ADVANCED MATERIALS & PROCESSES，2009 Oct
4. **Chien-Yu Chen**、Yea-Huey Chang、Da-Tian Bau、Hung-Jin Huang、Fuu-Jen Tsai*、Chang-Hai Tsai*、Chen, Calvin Yu-Chian*，Ligand-Based Dual Target Drug Design for H1N1: Swine Flu- A Preliminary First Study，JOURNAL OF BIOMOLECULAR STRUCTURE &

DYNAMICS，2009 Oct，27(2):171-178

5. **Chien-yu Chen**、Yea-huey Chang、Da-Tian Bau、Hung-jin Huang、Fuu-Jen Tsai*、Chang-Hai Tsai*、Chen, Calvin Yu-Chian*，Ligand-based design for heat shock protein 90 inhibitors，Surface Science，2009 Oct
6. **Chien-Yu Chen**、Da-Tian Bau、Yea-Huey Chang、Yuan-Man Hsu、Tin-Yun Ho、Hung-Jin Huang、Fuu-Jen Tsai*、Chang-Hai Tsai*、Chen, Calvin Yu-Chian*、Yu-An Chang，Drug design for Influenza A virus subtype H1N1，JOURNAL OF THE CHINESE INSTITUTE OF CHEMICAL ENGINEERS，2009 Oct
7. **Chien-Yu Chen**、Da-Tian Bau、Ming-Hsui Tsai、Yuan-Man Hsu、Tin-Yun Ho、Hung-Jin Huang、Yea-Huey Chang、Fuu-Jen Tsai*、Chang-Hai Tsai*、Chen, Calvin Yu-Chian*，Is That Possible to Design the Versatile Inhibitors for H1N1, H5N1, H5N2, and H5N7 ?，IEEE/ACM Transactions on Computational Biology and Bioinformatics，2009 Oct
8. **Chien-Yu Chen**、Da-Tian Bau、Ming-Hsui Tsai、Yuan-Man Hsu、Tin-Yun Ho、Hung-Jin Huang、Yea-Huey Chang、Fuu-Jen Tsai*、Chang-Hai Tsai*、Chen, Calvin Yu-Chian*，Drug Design for the Influenza A Virus Subtype H1N1，IEEE/ACM Transactions on Computational Biology and Bioinformatics，2009 Oct

9. Hung-Jin Huang、Da-Tian Bau、Ming-Hsui Tsai、Yuan-Man Hsu、Tin-Yun Ho、**Chien-Yu Chen**、Yea-Huey Chang、Fuu-Jen Tsai*、Chang-Hai Tsai*、Chen, Calvin Yu-Chian*，Dual-targeted Drug Design of HER2 and HSP90 by CoMFA Model and Pharmacophore Analysis，IEEE/ACM Transactions on Computational Biology and Bioinformatics，2009 Oct

10. **Chien-Yu Chen**、Da-Tian Bau、Ming-Hsui Tsai、Yuan-Man Hsu、Tin-Yun Ho、Hung-Jin Huang、Yea-Huey Chang、Fuu-Jen Tsai*、Chang-Hai Tsai*、Chen, Calvin Yu-Chian*，Drug Design for KU86 in DNA Break Repair System，IEEE/ACM Transactions on Computational Biology and Bioinformatics，2009 Oct

11. **Chien-Yu Chen**、Fuu-Jen Tsai、Jing-Gung Chung、Chang-Hai Tsai、Yuan-Man Hsu、Hung-Jin Huang、Tin-Yun Ho、Yea-Huey Chang、Da-Tian Bau*、Ming-Hsui Tsai*、Chen, Calvin Yu-Chian*，A Novel Strategy for Designing Dual-target Inhibitors of KU86 and XRCC4，IEEE/ACM Transactions on Computational Biology and Bioinformatics，2009 Oct

12. Yea-Huey Chang、Da-Tian Bau、Ming-Hsui Tsai、Yuan-Man Hsu、Tin-Yun Ho、**Chien-Yu Chen**、Hung-Jin Huang、Fuu-Jen Tsai*、Chang-Hai Tsai*、Chen, Calvin Yu-Chian*，Reducing without Side

Effects? A Novel Strategy for Designing the PPAR Agonists，IEEE/ACM Transactions on Computational Biology and Bioinformatics，2009 Oct

13. Hung-Jin Huang、Da-Tian Bau、Ming-Hsui Tsai、Yuan-Man Hsu、Tin-Yun Ho、**Chien-Yu Chen**、Yea-Huey Chang、Fuu-Jen Tsai*、Chang-Hai Tsai*、Chen, Calvin Yu-Chian*，What is the Key Point for Designing HER2 Inhibitors ?，IEEE/ACM Transactions on Computational Biology and Bioinformatics，2009 Oct
14. **Chien-Yu Chen**、Da-Tian Bau、Ming-Hsui Tsai、Yuan-Man Hsu、Tin-Yun Ho、Hung-Jin Huang、Yea-Huey Chang、Fuu-Jen Tsai*、Chang-Hai Tsai*、Chen, Calvin Yu-Chian*，Drug Design for AMP-Activated Protein Kinase Agonists in Silico，IEEE/ACM Transactions on Computational Biology and Bioinformatics，2009 Oct
15. **Chien-Yu Chen**、Da-Tian Bau、Ming-Hsui Tsai、Yuan-Man Hsu、Tin-Yun Ho、Hung-Jin Huang、Yea-Huey Chang、Fuu-Jen Tsai*、Chang-Hai Tsai*、Chen, Calvin Yu-Chian*，Could Traditional Chinese Medicine Used for Curing Erectile Dysfunction ?，IEEE/ACM Transactions on Computational Biology and Bioinformatics，2009 Oct
16. **Chien-yu Chen**、Yea-huey Chang、Da-Tian Bau、Hung-jin Huang、Fuu-Jen Tsai*、Chang-Hai Tsai*、Chen, Calvin Yu-Chian*，Discovery the

inhibitors of H5N1, H5N2, and H5N7 by pharmacophore analysis，Surface Science，2009 Oct

6-2. 研討會發表 Conference publications

1. Discovery the triple inhibitors of H5N1, H5N2, and H5N7 by pharmacophore analysis，20th International Conference on Adaptive Structures and Technologies (ICAST 2009)，香港，2009.10.20 ~ 2009.10.22
2. Is That Possible to Design the Versatile Inhibitors for H1N1, H5N1, H5N2, and H5N7 ?，2nd International Conference on BioMedical Engineering and Informatics (BMEI'09)，Tianjin, China，2009.10.17 ~ 2009.10.19
3. Could Traditional Chinese Medicine Used for Curing Erectile Dysfunction ?，2nd International Conference on BioMedical Engineering and Informatics (BMEI'09)，Tianjin, China，2009.10.17 ~ 2009.10.19
4. Drug Design for KU86 in DNA Break Repair System，2nd International Conference on BioMedical Engineering and Informatics (BMEI'09)，Tianjin, China，2009.10.17 ~ 2009.10.19
5. Drug Design for the Influenza A Virus Subtype H1N1，2nd International Conference on BioMedical Engineering and Informatics (BMEI'09)，Tianjin, China，2009.10.17 ~ 2009.10.19

6. A Novel Strategy for Designing Dual-target Inhibitors of KU86 and XRCC4，2nd International Conference on BioMedical Engineering and Informatics (BMEI'09)，Tianjin, China，2009.10.17 ~ 2009.10.19
7. Virtual Screening from the Maybridge Database and Molecular Docking Approach on Discovery of H5N1 Inhibitors，IEEE 2009 International Conference on Complex, Intelligent and Software Intensive Systems，Fukuoka Institute of Technology (FIT), Japan，2009.3.16 ~ 2009.3.19
8. Discovery the potent inhibitors of H5N1 by pharmacophore comparison analysis，第二屆中國醫藥大學暨亞洲大學生物科技研討會，立夫 B1 國際會議廳，2009.3.19 ~ 2009.3.19
9. Development a novo inhibitor of diarrhea from ginger components by virtual screening technique，第二屆中國醫藥大學暨亞洲大學生物科技研討會，立夫 B1，2009.3.16 ~ 2009.3.16
10. Discovery the potent inhibitors for phosphodiesterase 5 by multiple linear regression QSAR model prediction，第二屆中國醫藥大學暨亞洲大學生物科技研討會，立夫 B1 國際會議廳，2009.3.16 ~ 2009.3.16
11. Discovery the Potent Inhibitors for Phosphodiesterase 5 by Virtual Screening and Pharmacophore Analysis，13th Biochemical Engineering conference，元智大學，2008.6.27 ~ 2008.6.29
12. Structure Based and Phamacophore Analyses of Drug Resistance of Chicken Influenza A Virus (H5N1)，第一屆中國醫藥大學生物科技研

討會，中國醫藥大學，2008.4.7～2008.4.7

13. Components of Epimedium sagittatum and its derivatives could inhibit PDE5 activity in the view of computer-aided drug design，Symposium of Bioinformatics and Systems Biology in Taiwan，中正大學，2007.9.3～2007.9.5